Oxidative Modification of Vesicular Transporters in an Animal Model of Alzheimer's Disease

By

Ying Wang

A Thesis submitted to the Faculty of Graduate Studies of

The University of Manitoba

in partial fulfillment of the requirements of the degree of

MASTER OF SCIENCE

Department of Pharmacology and Therapeutics

University of Manitoba

Winnipeg, Canada

ABSTRACT

Oxidative stress is one of the major characteristics in Alzheimer's disease, and converging evidence indicates that cysteine S-nitrosylation might be related in AD pathology. My results demonstrated exogenous S-nitrosoglutathione was able to S-nitrosylate vAChT, vMAT2, vGluT1 and vGluT2. S-nitrosylation of these vesicular transporters inhibited the uptake of [^{3}H]acetylcholine, [^{3}H]dopamine and [^{3}H]glutamate respectively.

APP/PS1 transgenic mice were used to investigate neurotransmission dysfunctions of Alzheimer's disease. Global protein S-nitrosylation was increased in the 9 and 12 month APP/PS1 mice. Further investigation demonstrated an increase of vAChT and vGluT1 S-nitrosylation in frontal cortex of 6, 9 and 12 month APP/PS1 mice and an increased vAChT and vGluT1 S-nitrosylation was found in hippocampus of 3 month APP/PS1 mice.

These findings together suggest that S-nitrosylation of vesicular transporters inhibits the uptake of neurotransmitters, and S-nitrosylation of vAChT and might be associated with the neurotransmission dysfunction of acetylcholine and glutamate in Alzheimer's disease.

ACKNOWLEDGEMENTS

I am deeply indebted to Dr. Jun-Feng Wang. Without his guidance, support and good nature, I would never have been able to pursue neuroscience as a career. His experience of being a scientist helped me through three important years of my life.

I would also like to appreciate Dr. Fiona Parkinson and Dr. Eftekhar Eftekharpour for agreeing to be on my thesis committee despite their extremely busy schedule. I am tremendously grateful for their guidance and support on my project, and suggestions on my thesis writing. Without their efforts and kindness, this work would not have been done.

And I would like to thank all my colleagues who helped me get through three years of graduate school. Our research associate and my good friend Dr. Hua Tan, thank you for helping me arrange everything when I first came to Winnipeg and thank your for every convenience that you gave me for my experiments! Also I would like to thank the graduate students Zhu Zhou and Veni Bharti for sharing me with the personal experimental experience. It is a great experience to work with all of you! I would also like to thank our summer student Tarik Leylek for helping me with my cell culture in the summer time.

I would like to thank our collaborator Dr. Xin-Min Li and his graduate student Shenghua Zhu for sharing me the experience of maintaining the transgenic mice as well as experience of behavior tests.

Many thanks go out to my friends in the University – Junhui Wang, Jia Wang, Ruoyang Shi, Wenyan Li, Xiaosha Zhang, Lauren Roberts, Adam Hogan Cann, Hieu Nguyen and Dr. Yingxia Sun. I would also like to appreciate my best friend Yuting Wang for her endless courage during my stay in Canada. These individuals always helped me to keep my life in context. Graduate school isn't the most important thing in life, but good friends, good times and happiness are.

At the very end, I would like to appreciate my parents and Carol for their love and unconditional support during my study in Canada.

This project is supported by research fundings Canadian Institutes of Health Research (CIHR) and Manitoba Health Research Council (MHRC).

TABLES OF CONTENTS

LIST OF FIGURES

LIST OF ABBREVIATIONS

2DE	Two-Dimensional Electrophoresis
4-HNE	4-Hydroxynonenal
AD	Alzheimer's disease
AICD	APP Intracellular Domain
AMPA	α-Amino-3-hydroxy-5-Methyl-4-isoxazolepropionic Acid
APH-1	Anterior PHarynx-defective 1
ApoE	Apolipoprotein E
APP	β-amyloid precursor protein
Aβ	β-Amyloid
BACE1	β-site APP-Cleaving Enzyme
Cdk5	Cyclin-Dependent Kinase-5
cGMP	cyclic Guanosine Monophosphate
Drp1	Dynamin-related protein 1
eNOS	endothelial Nitric Oxide Synthase
ER	Endoplasmic Reticulum
FAD	Flavin Adenine Dinucleotide
FMN	Flavine Mononucleotide
GABA	γ-Aminobutyric Acid
GC	Guanylate Cyclase
GSH	Glutathione
GSK3β	Glycogen Synthase Kinase 3β
GSNO	S-Nitrosoglutathione
GSNOR	S-Nitrosoglutathione Reductase
GTPase	Guanosine Triphosphatase
HEK	Human Embryonic Kidney
IDE	Insulin Degrading Enzyme
iNOS	inducible Nitric Oxide Synthase
LC-MS	Liquid Chromatography-tandem Mass Spectrometry
LDL	Low Density Lipoprotein
LRP1	Lipoprotein Receptor-related Protein 1
LTP	Long Term Potentiation
MARK	Mitogen-Activated Protein Kinase
METH	Methamphetamine

MWM	Morris Water Maze
MCI	Mild Cognitive Impairment
NADPH	Nicotinamide Adenine Dinucleotide Phosphate
NET	Norepinephrine Transporter
NFT	Neurofibrillary Tangles
NMDA	N-Methyl-D-Aspartate
nNOS	neuronal Nitric Oxide Synthase
NO	Nitric Oxide
NOS	Nitric Oxide Synthase
PDI	Protein Disulfide Isomerase
PEN-2	Presenilin ENhancer 2
PS1	Presenilin 1
PS2	Presenilin 2
RNS	Reactive Nitrogen Species
ROS	Reactive Oxygen Species
sAPPα	Soluble Alpha Amyloid Precursor Protein
sAPPβ	Soluble beta Amyloid Precursor Protein
SMTC	S-Methyl-L-Thiocitrulline
SNAP25	Synaptosomal-Associated Protein 25
SNAREs	Soluble NSF Attachment Protein REceptors
SOD	Superoxide Dismutase
TBZ	Tetrabenazine
TBZOH	Dihydrotetrabenazine
TGN	Trans-Golgi-network
Trx	Thioredoxin
TrxR	Thioredoxin Reductase
vAChT	vesicular Acetylcholine Transporter
vATs	vesicular Amine Transporters
vGluT	vesicular Glutamate Transporters
vIAAT	vesicular Inhibitory Amino Acid transporter
vMATs	vesicular Monoamine Transporter
WEBGESTALT	WEB-based Gene SeT AnaLysis Toolkit
αCTF	Alpha Carboxyl Terminal Fragment
βCTF	β C-Terminal Fragment

CHAPTER 1: INTRODUCTION

1.1 Introduction of Alzheimer's Disease

Alzheimer's disease (AD) was first described by Dr. Alois Alzheimer for the demented female patient, Auguste D. in 1906. Over the past one hundred years, it has become the most common and the leading cause for dementia in the aged population, accounting for an estimated 60-80% of all cases [1]. It is reported that in the United States, approximately 5 million people now are suffering from AD, with a prediction of 50% increase by the year of 2025 [2]. AD is recognized as a neurodegenerative disorder. Tremendous amounts of cell injury and loss have been found in various parts of the brain, particularly in the hippocampus and neocortex of patients with AD [3]. One of most common characteristics in AD pathogenesis is that synaptic deficits could be observed before cellular death, which attributes to intellectual and cognitive declines in AD patients [4,5]. Yet the cause of AD is not fully understood. In all the cases, a majority of AD patients are sporadic, which is not contributed by heritance, while the other small proportion of the patients is familial, mainly related to three genes: β-amyloid precursor protein (APP), presenilin 1 (PS1) and presenilin 2 (PS2) [6]. AD patients might experience memory loss, cognitive impairments and behavioral changes like aphasia, apraxia, agnosia and executive dysfunction. Still there is no cure for this disease. Irrespective of genetics, advancing age is the leading cause to AD pathology, with the fact that people over 65 years of age are more vulnerable to get the disease.

1.2 Neuropathology of Alzheimer's Disease

Although the clear mechanisms of AD are not fully understood, Aβ plaques, neurofibrillary tangles (NFTs) and deficits of neurotransmitter systems have been identified to be the main pathological factors of AD [6,7,8].

1.2.1 Aβ Hypothesis

β-amyloid (Aβ) plaques result from aggregation of Aβ peptides that originate from cleavage of APP by β-secretase and γ-secretase [6]. Three major alleles of APP gene, located on chromosome 21, are responsible for the production of APP695, APP751 and APP770 (containing 695, 751, and 770 amino acids, respectively) [9], in which APP695 is predominantly expressed in neurons [10,11]. APP751 and APP770 are mainly responsible for senile plaques in the skin. The gene splicing with APP production in the brain suggests APP RNA dysregulation may contribute to pathogenesis of AD [12]. In APP family, though APP subtypes share some common conserved domains such as E1, Aβ domain is unique in each APP protein. APP is able to undergo rapid transport in neurons. In most of the cases, APP is transported from endoplasmic reticulum (ER) and then through trans-Golgi-network (TGN) facilitated by kinesin-I, finally onto cell membrane [13], where APP can be metabolized by α-, β- and γ-secretases to produce various products with different functions.

Multiple sites in APP can be recognized and then cleaved by specific secretases (Fig 1). APP in neurons can be first cleaved by either endoprotease α-secretase or β-secretase and then by another endoprotease γ-secretase [14]. γ-secretase is a protease made up of nicastrin, anterior pharynx-defective 1 (APH-1), presenilin enhancer 2 (PEN-2), and PS 1 or PS2 [15]. The cleavage site for α-secretase is at the Lys16-Leu17 bond (within Aβ domain), with the products of soluble α amyloid precursor protein (sAPPα) and α carboxyl terminal fragments (αCTF) [16,17]. αCTF can be further cleaved by γ-secretase to produce the small peptide p3 and APP intracellular domain (AICD). sAPPα plays important roles in neuronal plasticity and neuronal survival and it has protective properties against neuronal excitotoxicity [18,19]. Recently it is reported AICD can facilitate APP's intracellular trafficking and/or signal transduction by interacting with cytosolic factors. These interactions with different factors are normally controlled by the phosphorylation and de-phosphorylation of AICD [20]. AICD also has various roles in regulating transcription of multiple genes including *Glycogen Synthase Kinase-3β* (*GSK3β*), *KAI*1, *neprilysin*, *BACE1* (*β-site APP-Cleaving Enzyme*), *p53* and *LRP*1 (*Lipoprotein Receptor-related Protein* 1) [21-26]. P3 fragment, the other end-product comes from αCTF, will be degraded soon after cleavage and usually doesn't have any functions.

Alternatively, APP can be first cleaved by the β-secretase (BACE1), with the products of soluble ectodomain soluble beta amyloid precursor protein (sAPPβ) and β

C-terminal fragment (βCTF) [16,27]. The transmembrane domain on βCTF is then cleaved by γ-secretase, releasing Aβ and AICD. On βCTF, there are multiple cleavage sites for γ-secretase, leading to various metabolites, such as $A\beta_{1-40}$ and $A\beta_{1-42}$ [16]. sAPPβ differs from sAPPα by lacking the $A\beta_{1-16}$ region at its C-terminal. For the product functions, sAPPβ is reported to be a death receptor ligand, which could mediate axonal pruning and neuronal cell death [28]. The main end-products from βCTF are $A\beta_{1-40}$ and $A\beta_{1-42}$, standing for the number of amino acids within the Aβ peptides [16]. Recent studies have reported that Aβ participants in various signaling pathways, and also co-works with other risk factors in AD pathology [12,16,27,29-31]. Aβ toxicity mainly depends on several factors such as Aβ's peptide length, concentration and even conformational states [12,31]. Though the primary pathogenic event triggering synaptic loss and selective neuronal cell death in AD is still in debate, it is widely accepted that the most toxicity comes from Aβ oligomers, rather than insoluble fibrils. Basic units for Aβ oligomers are $A\beta_{1-40}$ and $A\beta_{1-42}$. $A\beta_{1-40}$ is the major product for β-secretase and γ-secretase cleavage, however, $A\beta_{1–42}$ monomers, under pathological conditions, are more prone to being aggregated and can be assembled into potential toxic oligomers [12, 29-31]. It has been reported that Aβ oligomers can cause synapse loss and neuronal death by disrupting various signaling pathways like fyn kinase, GSK3β and Cyclin-dependent kinase-5 (Cdk5) pathways [32]. Meanwhile, in a lot of studies, it is reported that Aβ can increase oxidative stress, hyperactivate N-methyl-D-aspartate (NMDA) receptors and contribute to mitochondrial dysfunction [33-36].

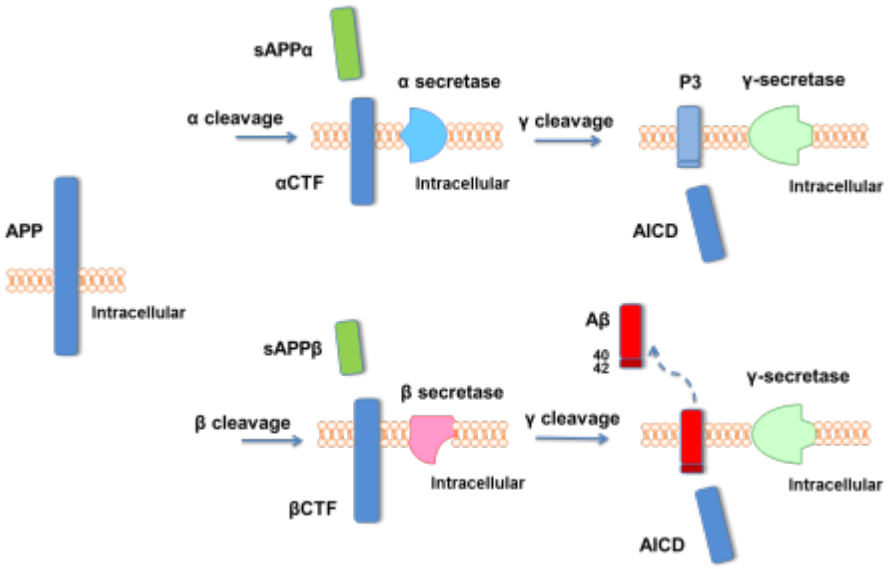

Figure 1. Metabolism of APP by secretases. APP can be cleaved in two pathways: the non-amyloidogenic pathway (upper) or amyloidogenic pathway (bottom). Abbreviations: APP-Amyloid Precursor Protein; sAPPα-Soluble Amyloid Precursor Protein α; sAPPβ-Soluble Amyloid Precursor Protein β; αCTF-α-secretase-cleaved C Terminal Fragment; βCTF-β-secretase-cleaved C Terminal Fragment; AICD-Amyloid Precursor Protein Intracellular Domain.

1.2.2 Tau Hypothesis

Another hallmark of the disease is NFTs that result from hyperphosphorylation of tau proteins in the neurons [37]. Tau proteins are expressed in axons and normally they bind to tubulin to stabilize microtubules. In AD pathology, tau hyperphosphorylation is supposed to be closely related to Aβ toxicity. In neurons, Aβ can increase the activity of different kinases including Mitogen-Activated Protein Kinase (MARK), GSK3β, and Cdk5 [38]. The increased activity of these kinases will hyperphosphorylate tau proteins, leading to disassociation of tau proteins from microtubules [7,8,38]. The disassociated tau proteins will then aggregate into non-filamentous inclusions such as toxic NFT, and

neurotoxic neuritic plaques [38]. The NFTs thus destabilize microtubules, causing impairments in axonal transport and neuronal dysfunction [7,8,38].

1.2.3 Cholinergic and Glutamatergic Dysfunctions in Alzheimer's Disease

In AD, the dysfunction of cholinergic and glutamatergic systems is implicated in the progression of AD [43]. Degeneration and loss of trophic support for the cholinergic neurons of the basal forebrain is one of the hallmarks of early AD patients [44]. The cholinergic deficits lead to decreased synthesis of acetylcholine [45]. In human brains, acetylcholine is an essential neurotransmitter in CNS and PNS that modulates multiple cognitive processes including selective attention, sensory input and associative thinking [46,47]. These functions are largely supported by the projections from cholinergic nuclei in the basal forebrain into virtually all cortical areas. However, they are severely damaged in early stage of AD [48,49]. It is also evidenced that cholinergic deficits might contribute to amyloid deposition and plaque formation [44].

Glutamate is the main excitatory neurotransmitter in CNS and PNS, which is involved in many processes such as long term memory. The glutamate receptors are divided into AMPA (α-Amino-3-hydroxy-5-methyl-4-isoxazolepropionic acid) and NMDA receptors, both of which are ligand-gated ion channels. AMPA is permeable to cations including Na^+ and K^+ as well as a small amount of Ca^{2+}, while NMDA is the main channel that is permeable to Ca^{2+} [50,51]. For a long term potentiation (LTP),

constant glutamate signaling is required to activate NMDA receptors on the post-synaptic terminals [52,53], which is an important hypothesis of long term memory. In AD, chronic, mild activation of NMDA receptors ultimately leading to neurodegeneration is one of the main symptoms for neurotransmission imbalance termed excitotoxicity [50,54]. Hyperactivation of glutamate receptors (NMDA receptors) allows the influx of Ca^{2+} ions into postsynaptic neurons, leading to increased nitric oxide (NO) production, increased free radicals, calcium homeostasis dysfunction, activation of proteases, increased cytotoxic transcription factors and neuronal cell death [55,56].

The dysfunction of cholinergic and glutamatergic systems as well as other neurotransmitter systems contribute to the cognitive changes and neuropathology of AD. Therefore, a large category of current available drugs on the market for mild to moderate stage of AD are used to enhance acetylcholine level in the brain, for instance, donepezil, rivastigmine and galantamine [57]. Second generation drug memantine is also used as a non-competitive antagonist to block the hyperactivity of NMDA receptors caused by glutamate [56,57].

1.3 APP/PS1 Animal Model in Alzheimer's Disease Research

In human patients, AD is characterized by memory loss, cognitive impairments and behavioral changes like aphasia, apraxia, agnosia and executive dysfunction. However, with the limitation of human study, the recent understanding of AD pathology

tremendously comes from AD transgenic animal models. Within these models, APP/PS1 model is largely used, mainly focusing on mimicking amyloid plaques. It provides useful and practical platforms for understanding the role of Aβ in AD pathogenesis.

APP/PS1 mice express a chimeric mouse/human APP (K670N/M671N Swedish mutations) and a mutant human PS1 (M146L) controlled by prion promoter elements [60] (Fig 2). $APP_{K670N/M671N}/PS1_{M146L}$ mice were generated by crossing $APP_{K670N/M671N}$ single transgenic mice with $PS1_{M146L}$ single transgenic mice [60]. The amount of fibrillogenic $A\beta_{1-42}$ species produced is 5 times higher by 6 month of age than the control group [60].

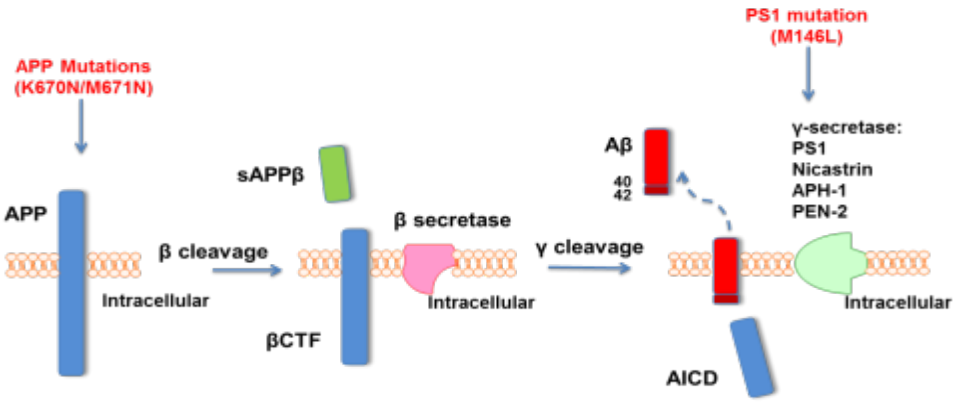

Figure 2. Gene mutations of APP/PS1 animal model. APP/PS1 mice overexpress a chimeric mouse/human APP K670N/M671N Swedish mutations and a mutant human PS1 carrying M146L. Abbreviation: APH-1-Anterior PHarynx-defective 1, PEN-2-Presenilin Enhancer 2.

Behavioral deficits have also been widely reported in the APP/PS1 transgenic mouse model. A review of the literature shows that APP/PS1 mice exhibit a number of

cognitive deficits detected by elevated plus maze (EPM), T maze, Y-maze and Morris Water Maze (MWM). The damage of spatial memory is one of the main cognitive changes detected in this model, and the damage could be detected as early as 6 month of age [61-68]. Short term memory loss was also reported as early as in 3 month in a T maze test [69]. Significant increased level of anxiety was also detected in the elevated plus maze and open field test in young and old transgenic mice [51]. The APP/PS1 double transgenic mice also tended to be more active than the wild type mice, which might be related to the aggressive behaviors caused by AD [61,70]. Though this model cannot fully mimic AD symptoms in human being, it does provide researchers with various materials to investigate mechanisms of AD pathology, and develop therapeutic agents.

1.4 Introduction of Oxidative Stress

Reactive oxygen species (ROS) and reactive nitrogen species (RNS) are a series of molecules that contain one or two unpaired electrons. Among these reactive molecules, hydroxyl radical (OH), superoxide, nitric oxide (NO), peroxnitrite ($ONOO^-$), transition metals (copper and iron), 4-Hydroxynonenal (4-HNE) are the most abundant species [71]. Under physiological conditions, ROS production is balanced by innate antioxidant system, which consists of chemical substances and enzymes such as superoxide dismutase (SOD), glutathione (GSH), glutathione peroxidase, thioredoxin (Trx) and

others. However, when the antioxidant system is overwhelmed by the increased oxidative stress, overproduced ROS causes oxidative damage to DNA, lipids and proteins [78,79,142]. ROS and RNS such as hydrogen peroxide, hydroxyl radicals, 4-HNE and peroxynitrite can further oxidatively modify proteins, including carbonylation, nitration, oxidation and S-nitrosylation of the proteins, which might alter protein structures, silent enzymatic activity, or interference with regulatory protein interactions [72]. Therefore, oxidative protein modification may result in changes of protein activity, alteration of protein-protein interactions, abnormal protein aggregation and apoptosis.

1.4.1 Oxidative Stress in Alzheimer's Disease

Increasing evidence suggests that oxidative protein modification significantly contributes to pathophysiological development of AD [73]. Since AD is an age-dependent disease and mainly occurs in elderly people over 65 years old (except for familial patients), ageing is a leading factor for the disease. The free radical theory is a very important hypothesis of aging, which demonstrates that accumulated oxidative damage by overproduction of free radicals over time due to deficits of antioxidant systems [74,75]. Overproduced ROSs cause various oxidative damages in AD [76,77]. Interestingly, more and more studies have reported that AD brains exhibit increased oxidative/nitrosative stress [78]. And within all kinds of oxidative damage, emerging

evidence suggests that oxidative protein S-nitrosylation significantly contributes to pathophysiological development of AD [79].

1.5 Nitric Oxide and Protein S-Nitrosylation

NO is produced from L-arginine catalyzed by nitric oxide synthases (NOS) including endothelial NOS (eNOS), neuronal NOS (nNOS) and inducible NOS (iNOS) [80-82]. This process also requires cofactors/coenzymes such as nicotinamide adenine dinucleotide phosphate (NADPH), flavine mononucleotide (FMN) and flavin adenine dinucleotide (FAD) [83,84]. The actions of NO are multifaceted mainly classified into two categories including the classic cyclic guanosine monophosphate (cGMP) dependent actions and cGMP-independent actions [85]. Studies have shown that NO at nanomolar concentrations are sufficient enough to activate guanylate cyclase (GC) and then trigger cGMP-dependent signals. NO-activated cGMP has been recognized to play critical roles in NO-mediated vasodilation [86], in various cellular signaling pathways to regulate a spectrum of brain functions such as neuronal developments, synaptic plasticity, and apoptosis [87], and contributes to immune system, neurotransmission process and regulation of cardiac contractility [88-90].

NO at higher than 50-100 μM can attack thiol groups of cysteine residues in proteins via covalently binding and induce protein cysteine S-nitrosylation [91-94]. Cysteine residues in proteins are critical in regulating enzymes, transcription factors,

protein structures and metal binding [95-98]. Thiols of cysteine residues are very susceptible to the attack by NO radicals. Like other posttranslational modifications, S-nitrosylation is able to trigger the conformational changes of various types of proteins.

In AD, nitrosative post-translational modifications of proteins are significantly increased mainly by cysteine S-nitrosylation [85,100-105], which is attributed to the overproduction of NO. In central nervous system of AD patients, NMDA glutamate receptors play a central role in the regulation of NO production [105]. The main resources of NO are coming from two major pathways. First, the hyperactivity of NMDA receptors caused by Aβ toxicity results in an increased Ca^{2+} influx. Increased intracellular calcium then activates nNOS and increases NO production [106-108]. Second, Aβ oligomers can activate iNOS in glial cells, generating high levels of NO [87,106,109]. The high amount of NO in AD brains might target a wide variety of proteins. Indeed studies have presented compelling evidence implicating that S-nitrosylation of proteins is involved in the pathogenesis of AD [33,110,111].

1.5.1 The Role of S-Nitrosylation in Alzheimer's Disease

Many studies have shown that S-nitrosylation of various proteins is increased in the brains of AD patients. Although the exact mechanisms of increased S-nitrosylation remain largely unknown, the vast majority of S-nitrosylated proteins are reported to be

involved in Aβ production, mitochondrial dysfunction protein misfolding and synaptic loss.

1.5.2 Protein S-Nitrosylation on Aβ Production

BACE1, insulin-degrading enzyme (IDE) and apolipoprotein E (ApoE) are three factors that regulate Aβ metabolism and aggregation. *In vitro* studies have shown that all of these three proteins can be S-nitrosylated in cell models, and increased S-nitrosylation of BACE1, IDE and ApoE can also be found in AD post mortem brains, suggesting a relationship between S-nitrosylation proteins and Aβ deposition.

BACE1 together with γ-secretase cleaves transmembrane APP to form Aβ peptides. Since BACE1 is essential for Aβ production, the expression and enzymatic activity of BACE1 can change Aβ deposit. Young et al. found that NO donor S-nitrosocysteine (SNOC) at 100 nM and higher concentrations increased S-nitrosylation of BACE1 in primary cultured cortical neurons [85]. They also found that S-nitrosylation of BACE1 inhibits its activity, in which the Aβ content was found significantly lower at both 100 nM and higher doses of SNOC [85]. Interestingly, BACE1 S-nitrosylation in AD brains was higher in Mild Cognitive Impairment (MCI) stage than in late AD stage, which inversely correlates with BACE1 protein levels [85]. These findings together demonstrated a suppressive effect on Aβ load from S-nitrosylation of BACE1.

IDE is a conserved zinc metalloprotease (M16 family) that is responsible for the clearance of various hormones and peptides, including insulin and Aβ [112]. It is evidenced that the NO donor S-nitroso-N-acetylpenicillamine (SNAP) could increase S-nitrosylation of purified rat IDE enzyme [113]. In another study, Cys110, Cys178, Cys789, Cys819 and Cys966 residues of IDE were identified to be S-nitrosylated in the human IDE transfected HEK 293T cells [114]. Further study demonstrated that S-nitrosylation of Cys110 and Cys819 leads to complete inactivation of IDE, while S-nitrosylation of both Cys789 and Cys966 together also causes conformational change and aggregation of IDE, resulting in the inhibition of IDE activity [114]. Both of these two studies found various NO donors could also significantly reduce IDE enzyme activity, which is presented with a lower efficiency in insulin and Aβ degradation [113,114]. This result suggests a potential role of S-nitrosylation on IDE function and Aβ production. Since IDE is a very important modulator for Aβ production, inhibition of IDE activity by NO in the brain may increase the accumulation of Aβ, leading to neuronal cell death.

ApoE represents a family of proteins including ApoE2 ApoE3 and ApoE4, which are expressed in the brain [115]. ApoE is essential for the normal catabolism of triglyceride-rich lipoprotein metabolites. ApoE isoforms also enhance the break-down of Aβ both within and between cells, while ApoE4 is not as effective as the others at promoting these reactions. Therefore gene variation of ApoE4 normally results in

increased vulnerability to AD, making it one of the important genetic risk factors for AD pathology [116]. Alexander et al reported the S-nitrosylation of ApoE2 and ApoE3, but not the ApoE4 is increased in the HEK-293 cell line transiently transfected with NOS1, suggesting that ApoE2 and ApoE3 can be S-nitrosylated. Specifically, Cys112 and Cys158 in ApoE2 and Cys112 in ApoE3 were identified as S-nitrosylation sites [117]. S-nitrosylation of ApoE2 and ApoE3 inhibits the binding of ApoE to low density lipoprotein (LDL) receptors [117]. Since the activities of the ApoE isoforms are essential for the break-down of Aβ, the inhibitory effect caused by S-nitrosylation on ApoE2 and ApoE3 may potentially increase Aβ deposit, contributing to AD pathology.

Aβ plaques, as one of the most important pathological hallmarks in AD, contribute to NMDA receptor hyperactivity, synapse loss and neuronal cell death. NO might regulate Aβ production by S-nitrosylating Aβ-production-related proteins. In these findings, S-nitrosylation of BACE1 potentially suppresses Aβ production, showing a 'beneficial' effect, while S-nitrosylation of IDE and ApoE potentially increases Aβ production, showing a 'detrimental' effect. These results implicate a potential pharmaceutical way to reduce Aβ production either by S-nitrosylating beneficial proteins or de-nitrosylating detrimental proteins.

1.5.3 Protein S-Nitrosylation on Mitochondrial Dysfunction

Mitochondrion is the main site where the energy currency ATP is produced. Mitochondrial function and energy metabolism are impaired early in the course of Alzheimer's disease [35]. Recently it is reported that excessive S-nitrosylation of mitochondrial proteins might suppress the protein functions, thus compromising at least partially mitochondrial functioning, especially in neurodegenerative diseases such as AD, where ROS/RNS are overwhelmed in certain stages of the disease [78,186]. Within these S-nitrosylated proteins, S-nitrosylation of dynamin-related protein 1 (Drp1) is the most related to mitochondrial dysfunction in AD. Drp1, as a dynamin-related Guanosine Triphosphatase (GTPase), is responsible for mitochondrial division and involved in regulation of mitochondrial fission [36,118-121]. Dong et al reported that S-nitrosylation of Drp-1 was increased in mouse cerebrocortical cells treated with oligomeric $A\beta_{25-35}$ and in post mortem brains of patients with sporadic AD [110,122,123]. Furthermore, S-nitrosylation of Drp1 accelerates mitochondrial fragmentation and neuronal synaptic damage in HEK 293 cells [110], indicating S-nitrosylation of Drp1 may contribute to mitochondrial dysfunction in AD.

1.5.4 Protein S-Nitrosylation on Protein Misfolding

Protein misfolding and aggregation are increased in brain of patients with AD, for example, NFTs are caused by hyperphosphorylated tau aggregates, while Aβ plaques are

caused by Aβ aggregates [6,7,8]. Recent studies have shown that NO also promotes protein misfolding by S-nitrosylating protein disulfide isomerase (PDI). PDI catalyzes the correct formation of disulfide bond based on thiol-disulfide exchange reactions [124], and PDI also serves as a molecular chaperone that assists in the maturation, transport, and folding of secretory proteins [109]. Studies have reported that PDI S-nitrosylation is increased in post mortem brains of subjects with AD when compared to controls [125,126]. The researchers isolated PDI and S-nitrosylated PDI for the functional study, in which both chaperone activity and isomerase activity of S-nitrosylated PDI were decreased compared to normal PDI [126]. As the tremendous roles that PDI play in ER stress, it is suggested that S-nitrosylation of PDI might exacerbate ER stress, which may lead to cell death.

1.5.5 Protein S-Nitrosylation on Synaptic Loss

Neuronal dysfunction and degeneration is predominantly in the hippocampus and cerebrocortex of AD patients [3]. Cdk5 is a cyclin-dependent kinase has been implicated in multiple neuronal functions, including axon guidance, neuronal migration, neuronal survival and the regulation of synaptic spine density [127-129]. Cdk5 is reported to be an important modulator of NMDAR receptors in AD as it can be hyperactivated by a number of stimulus (e.g oxidative stress, Aβ exposure and calcium overload), contributing to neuronal cell death [130]. It is evidenced that NO donors could increase

S-nitrosylation of Cdk5 at Cys83 and Cys157 residues in transfected SH-SY5Y cells and the HEK293 cells [33]. Further investigation demonstrated that increased S-nitrosylation of Cdk5 increased its enzyme activity, leading to Aβ/NMDAR-mediated spine loss and the pathogenesis of AD [33].

1.5.6 Identification of S-Nitrosylated Proteins in AD Patients

Recently due to the development of high throughput proteomic techniques, many S-nitrosylated proteins are identified in AD post mortem brains or AD animal models. Identification of S-nitrosylated protein using the proteomic technique consists of three steps, including a classical biotin switch method being used to enrich S-nitrosylated proteins, two-dimensional electrophoresis (2DE) being used to separate S-nitrosylated proteins and Liquid chromatography-tandem mass spectrometry (LC-MS/MS) being used to identify individual S-nitrosylated proteins [34]. Studies using proteomic technologies revealed that many proteins can be S-nitrosylated in human AD post mortem brains, for example, including MAGUK, CamkII, or synaptotagmins [131]. WEB-based Gene SeT AnaLysis Toolkit (WEBGESTALT) and UniProt [34] show that the vast majority of S-nitrosylated proteins are related to synaptic loss, apoptosis, energy metabolism and redox regulation [34,131].

1.5.7 Antioxidants and Pharmacological Treatment for Protein S-Nitrosylation in Alzheimer's Disease

Oxidative stress is one of the main characteristics in Alzheimer's disease. NO can induce protein S-nitrosylation. Protein S-nitrosylation is known to be involved in mitochondrial dysfunction, protein misfolding, synapse loss and Aβ production and therefore may have either a direct or an indirect effect on AD pathology. These findings suggest that the process of S-nitrosylation could be a target for the pharmacological treatment of AD.

S-nitrosylated thiols in cysteine residues can be reduced back to free thiols by GSH and Trx along with their reductase [94]. S-nitrosylated thiol groups can be de-nitrosylated by GSH, forming a reduced protein thiol and S-nitrosoglutathione (GSNO). GSNO is rapidly and irreversibly metabolized by S-nitrosoglutathione reductase (GSNOR) to glutathione S-hydroxysulfenamide (GSNHOH). S-nitrosylated thiol groups can also be de-nitrosylated by Trx through its dithiol moiety to form thioredoxin disulfide ($TrxS_2$) and HNO or NO, while $TrxS_2$ can be metabolized by thioredoxin reductase (TrxR) [99].

Antioxidants that can scavenge the excessive NO within the brain may have potential for AD treatment involving S-nitrosylation. Polyphenolic compounds extracted from green tea, magnolia, blueberries and grapes scavenge ROS/RNS including NO and exhibit neuroprotective effects. Studies have shown that these compounds produce

beneficial effect on both *in vivo* and *in vitro* in animal models for AD [178-182]. Since inhibition of NOS can reduce NO production, NOS inhibitors may also be beneficial for AD treatment. NOS inhibitors 1400W (N-(3-(aminomethyl)benzyl)acetamidine), L-NIL (N-iminoethyl-L-lysine) and L-NAME (N-nitro-L-arginine methylester) were found not only to reduce NO release but also to inhibit Aβ and glutamate-induced neuronal cell death [183,184]. Other compounds were also found to produce a beneficial effect on AD pathology by inhibiting NOS activity. Rutin is a flavonoid that can dose-dependently decrease $A\beta_{42}$-induced cytotoxicity in human SH-SY5Y neuroblastoma cells. One of its main effects is to decrease NO production by reducing iNOS activity [185]. Ferulic acid ethyl ester was reported to protect neurons against $A\beta_{1-42}$-induced toxicity in primary neuronal cell culture in part by down-regulation of iNOS [186]. Xanthorrhizol reduced ROS generation and glutamate-induced neurotoxicity in the murine hippocampal HT22 cell line, partially by reducing the expression of iNOS, which consequently resulted in the reduction of NO [183].

NMDA receptors are now considered to be a target for AD treatment as it plays vital role in neuronal excitotoxicity. NMDA receptor activation can increase NO production and increased NO can then S-nitrosylate NMDA receptor, resulting in negative feedback regulation of NMDA receptor activity. Therefore, alteration of NMDA receptor status may also have a potential for AD treatment. Nitroglycerin, which donates NO, has been shown to limit excessive NMDA receptor activity in rat AD

models [184,187]. Nitromemantines are combinatorial drugs of memantine and NO donors. Theoretically memantine works as a homing molecule to allow NO donor to combine with S-nitrosylation sites of the NMDA receptor. Nitromemantines have been proven to be highly neuroprotective in cultured rat primary cortical neurons treated with Aβ [188].

1.6 Introduction of Vesicular Transporters

1.6.1 General Process of Neurotransmission and Uptake

Neurotransmission imbalance has long been recognized in AD pathology. And a number of studies have demonstrated that cognitive changes in AD patients are caused by progressive loss of cholinergic deficits in basal forebrain and the alterations of other neurotransmitters such as glutamate [39-41]. Neurotransmitters are synthesized by cytosolic enzymes, and then packed into synaptic vesicles. Different vesicular transporters are anchored in the membrane of synaptic vesicles and responsible for the packaging of different neurotransmitters into synaptic vesicles [42,134]. Then the neurotransmitter-containing vesicles travel to the active zones of presynaptic membrane for docking, which is mediated by soluble NSF attachment protein receptors (SNAREs) [42]. SNARE complex is composed of synaptobrevin, syntaxin and synaptosomal-associated protein 25 (SNAP25). During the docking process, synaptobrevin, syntaxin and SNAP25 together form a protein complex by protein-protein

interaction, which allows vesicular membrane to fuse with presynaptic membrane [42]. Fusion then triggers exocytosis and releases neurotransmitters into the synaptic cleft. Trafficking, docking and fusing of vesicles are calcium-dependent and also require ATP. The released neurotransmitters will react with the receptors on the dendrites of the next neuron. The neurotransmitters in the cleft will further be re-uptaken into the pre-synapses (5-HT, NE and so forth) or into the astrocytes [GABA (γ-Aminobutyric acid) and glutamate] or degraded by cholinesterase (acetylcholine) [42].

The uptake process of neurotransmitters by vesicles depends on H^+ electrochemical gradient. Vacuolar H^+-ATPase first uses the energy released by ATP hydrolysis to pump protons into the vesicle lumen, generating H^+ electrochemical gradient [132]. The transport of amines including monoamines and acetylcholine primarily depends on the chemical component, ΔpH; while the transport of glutamate, predominantly depends on the membrane potential ($\Delta\psi$) [134]. In addition to H^+ electrochemical driving force, the cytosolic concentration of transmitter and intrinsic properties of the vesicular transporter also regulate the uptake of neurotransmitters [132].

1.6.2 Classification of Vesicular Transporters

There are three families of vesicular transporters, including vesicular amine transporters (vATs), vesicular inhibitory amino acid transporter (vIAAT/vGAT) and vesicular

excitatory amino acid transporters (vEAATs/vGluTs) [71,73,132]. vAChT (vesicular acetylcholine transporter) is one type of vATs which is response for the uptake of acetylcholine. Vesicular Monoamine Transporters (vMATs) from vATs have two isoforms including vMAT1 and vMAT2, in which vMAT1 is restricted to endocrine cells and vMAT2 is mainly expressed in neurons [59]. vMATs are responsible for the uptake of monoamines into the synaptic vesicles, and the major difference between these two transporters is that vMAT1 does not transport histamine [132]. vGAT is the only isoform that is responsible for the uptake of GABA and glycine [73]. The glutamate uptake is modulated by vGluTs (vGluT1, vGluT2 and vGluT3) in the brain. vGluT1 and vGluT2 are predominant and expressed exclusively in the central nervous system [58,133], while the exact function of vGluT3 is still unknown. Specifically, vGluT1 is localized mainly in neocortex, entorhinal and piriform cortex, hippocampus amygdale and subiculum [134], and vGluT2 is mainly expressed in thalamus, midbrain, and brainstem [135].

1.6.3 Vesicular Transporters in Alzheimer's Disease

As the important roles that vesicular transporters play in neurotransmission process, studies have been focused on the expression changes of vesicular transporters. In AD, it is evidenced that vGluT1 is significantly reduced in temporal cortex and frontal cortex of the old APP/PS1 mice and 3xTg AD mice (APPswe, $PS1_{M146V}$, and tau_{P301L}), but the

expression of vGABA, vGluT2 remained unchanged [136-139]. Decreased expression of vAChT was also reported in the hippocampus of Aβ-injected mice [139] and in postmortem AD brain [140]. However, no direct evidence has been reported on the changes of vMAT expression in AD. Vesicular transporters are very important in AD for the following two reasons: First, the vesicular neurotransmitter transporters could be very great indicators for vesicle function. Second, the regulation of vesicular transporter abundance, location, and activity is now appreciated to play a major role in determining synaptic neurotransmission [138-140].

1.7 Overall Objectives of This Project

Studies have consistently shown that oxidative stress is increased at early stage in patients with AD and in AD animal models. Cognitive changes are the characteristics for AD patients, mainly caused by dysfunction of acetycholine and glutamate. Recently evidence has shown the vGluT1 and vAChT expression is closely related to the glutamatergic deficits in AD, however, the mechanism remained not clear. Excessive NO in AD has been verified to induce cysteine S-nitrosylation of several proteins in AD, and the changes of their protein functions are implicated to AD pathology. Therefore, we hypothesize that S-nitrosylation of vGluT1 and vAChT contributes to the glutamatergic and cholinergic dysfunction in AD. Our goals are to understand the role that S-nitrosylation of vesicular transporter plays on neurotransmitter uptake, and the

possible relationship between the S-nitrosylation of vAChT and vGluT1 and neurotransmission dysfunction in APP/PS1 animal model. Our objectives are as follows:

1. To determine whether vAChT, vMAT2, vGluT1 and vGluT2 can be S-nitrosylated.
2. To determine the effect of S-nitrosylation of vAChT, vMAT2, vGluT1 and vGluT2 on the uptake of acetylcholine, dopamine and glutamate.
3. To determine whether vAChT and vGluT1 are S-nitrosylated in APP/PS1 mouse model.

CHAPTER 2: MATERIALS AND METHODS

2.1 APP/PS1 Double Transgenic Mice and Genotyping

The APP /PS1 double transgenic mice used in this study were obtained from cross breeding single transgenic mice expressing human $APP_{K670N/M671L}$ with single transgenic mice expressing human $PS1_{M146L}$ [60]. The mouse colonies were kept and maintained in a pathogen free environment in the Central Animal Care Service (CACS) at the University of Manitoba. All procedures of animal study were in accordance with the guidelines from the Canadian Council on Animal Care.

APP/PS1 transgenic mice were selected by the genotyping using PCR. At 3 weeks after birth, mice were weaned and ear marked. 0.5 cm tissue sample was taken from the tail tip of each mouse. Tissues were then digested in 300 μl of lysis buffer (50 mM Tris-HCl pH 8.0, 1 mM EDTA pH 8.0, 20 mM NaCl, 1% SDS) containing 7 μl of 20 mg/ml protease K (Roche) at 55 °C overnight. Samples were centrifuged at 17,000 x g for 10 min and then supernatants were transferred to new tubes. DNA was precipitated by adding equal volume of cold 100% ethanol, followed by centrifugation at 17,000 x g for 10 min. Then the supernatant was discarded, and the pellets were washed twice in 70% ethanol and dried. DNA pellet was resuspended in 100 μl double distilled water. The human APP primers and human PS1 oligo primers were used for genotyping. Human APP: forward primer 5'-GCC GTT GAC AAG TAT CTC GAG ACA CCT GG-3'; reverse primer 5'-GTG TCT CCA CCA GCT GCT GTC TCT CGT TGG C-3';

Human PS1: forward primer 5'-GAC AAC CAC CTG AGC AAT AC-3'; reverse primer 5'-CAT CTT GCT CCA CCA CCT GCC-3'. As shown in Figure 3, APP and PS1 positive mice displayed two target bands, with 250 bp and 145 bp in size, while wild type mice displayed no bands. The animals were randomly to which treatment they receive. APP/PS1 mice and wild-type mice were grown up to 3, 6, 9 or 12 months.

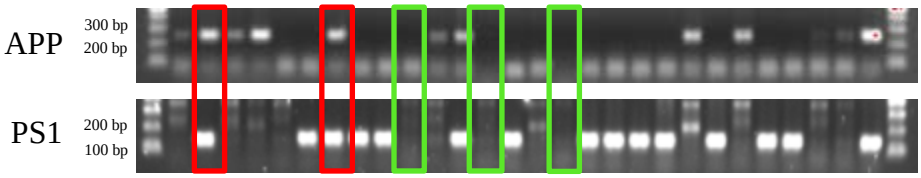

Figure 3. Genotyping of APP and PS1 genes in APP/PS1 and wild type mice. Totally 453 mice from 4 batches were genotyped for APP and PS1 genes respectively. APP positive band is 250 bp and PS1 positive band is 145 in size, while non-transgenic mice displayed no bands. The red boxes are examples of APP/PS1 mice, and green boxes are examples of wild type mice.

2.2 Behavior Tests

2.2.1 Locomotion Detection

Locomotor activity was evaluated by placing a mouse into a black Plexiglas (50x50x50 cm) open-field arena. Before testing, all the mice were handled in the colony room for 5 min daily for 5 days, and placed in the behavior room for at least 30 min before test. Warm red overhead lighting was put inside the room. During the test, the mouse was allowed to freely explore for 1 h [131,141,142]. Total distance traveled for 1h in the arena was recorded by a computer-operated digital camera and then analyzed

by EthoVision XT system (Noldus Information Technology Inc., Leesburg, VA, USA) (Fig 4A).

2.2.2 Y-Maze Spontaneous Alternation Test

Y maze spontaneous alternation test is used to detect the rodents' willingness to explore new environments based on the fact that rodents typically prefer to explore a new arm of the maze rather than the one they previously visited. Y maze is a test for short term memory. The mouse was put in the center of a Y-shaped maze with three white plastic arms at a 120° angle from each other and allowed to freely explore the three arms for 8 min (Fig 4B). The spontaneous alternation of entries and total arm entries were recorded. Spontaneous alternation for the mice was defined as the entry into each three consecutive arms in overlapping triplet sets [143,144]. The percent of spontaneous alternation was calculated by the percentage of non-repetitive triads in total triads.

2.2.3 Morris Water Maze Test

The Morris water maze was conducted in a circular tank, which is 145 cm in diameter and 60 cm high [145]. EthoVision XT system was used to track the movement of the mice throughout the experiment. The water level was approximately 50 cm high and the temperature was kept at 20-23 °C. The water tank was divided into 4 quadrants with 1 visual cue (different colors and shapes) in each quadrant of the water tank [145]. A PVC

square platform (10 x 10 cm) was located in one quadrant area and submerged in water with 0.5-1 cm below surface. The water was mixed with milk to block the vision of the platform. For the spatial training (learning process), the mice were trained to locate and escape onto the platform using distal cues for 4 trials per day with a 60s interval for 4 consecutive days. On each trial, the platform was fixed in the center of north east (NE) and the mice were placed in a different starting position [west (W), south (S), south east (SE) or north west (NW) of the maze] with facing the tank wall [145] (Fig 4C). Mice were allowed to swim for maximum 60 seconds (s). When animals could not find the platform within this time limit, they were guided to the platform. The animals were left on the platform for 30s in order to memorize the platform location. On day 5, the platform was removed. Then the mice were placed in the position which was 180° from the original platform position and allowed to swim for 60 s [145]. Latency to reach platform site and numbers of platform-site crossing during 60s were recorded. Swim speed and swim distance were also recorded and calculated.

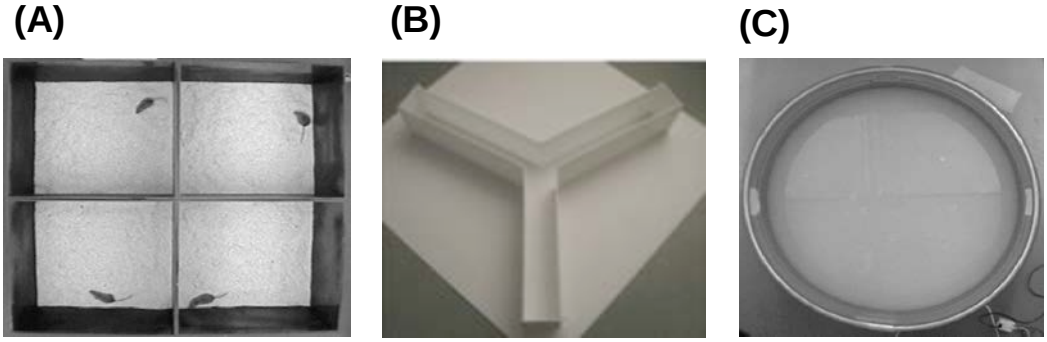

Figure 4. Behavioral apparatuses. (A) Calibration image of the open field apparatus as viewed in EthoVision XT system. The open field apparatus consists of a bare square box (50x50x50 cm). Four boxes were put together. A tracking camera was fixed above the

boxes. (B) Image of the Y maze apparatus. The length of arm is 35 cm, the height of arm is 10 cm and width of the arm is 5 cm. (C) Calibration image of the water maze pool as viewed in EthoVision XT system. A tracking camera was fixed above the tank to capture the movement of mice.

2.3 Tissue Processing and Protein Isolation

S-nitrosothiol groups within the proteins are light-sensitive, thus mouse brains were isolated in the room with dimmed light to protect the S-nitrosothiol groups from direct light, and all the following steps including dissection and protein isolation were also under this procedure. Mouse brains were dissected, and frontal cortex and hippocampus were isolated from each brain and stored in -80 °C freezer. Hippocampus and frontal cortex tissues were weighed and every 1 g of tissue was lysed with 10 ml Laemmli lysis buffer (20 mM Hepes pH 7.5, 250 mM NaCl, 20% glycerol, 30 mM $MgCl_2$, 0.5 mM EDTA, 0.1 mM EGTA, 1% nonide P40, 1 x protease inhibitors cocktail). Samples were then sonicated and kept on ice for 1h, followed by centrifugation at 10,000 x g for 15 minutes. The supernatant of each sample was transferred to a new tube. Protein concentrations of cell lysates were determined by using the bicinchoninic acid (BCA) method (Pierce, Rockford). Protein extract was aliquoted and stored in -20 °C.

2.4 Vesicle Isolation

The method for vesicle isolation was modified from Chu et al [146]. Mouse brains were homogenized in ice-cold buffer [0.32M sucrose, 5mM HEPES (pH 7.4), 1 x protease

inhibitors cocktail] (10 ml buffer per 1 g brain tissue) in glass tube homogenizer. Homogenate was then centrifuged at 1,000 x g for 10 minutes at 4 °C (Step 1). The supernatant was kept and then centrifuged at 20,000 x g for 30 minutes at 4 °C (Step 2). The pellets were collected and then subjected to osmotic shock by homogenization (10 strokes with Teflon pestle) in 10 ml/1 g tissue of distilled water. Osmolarity was restored by addition of an equal volume of 2 x HEPES and potassium tartrate buffer. Then the homogenate was centrifuged at 20,000 x g for 30 minutes at 4 °C (Step 3) and supernatant was collected. The equal amount of 2 mM $MgSO_4$ buffer was added to supernatant to get 1 mM $MgSO_4$ solution, which is then centrifuged at 100,000 x g for 1h at 4 °C (Step 4) [146]. The pellets were re-suspended in 0.32M sucrose (dissolved in assay buffer) or assay buffer, and stored in the -80 °C freezer. The enrichment of vesicles was verified by western blot using anti-vGluT1 antibody and anti-SNAP-25 antibody (Fig 5).

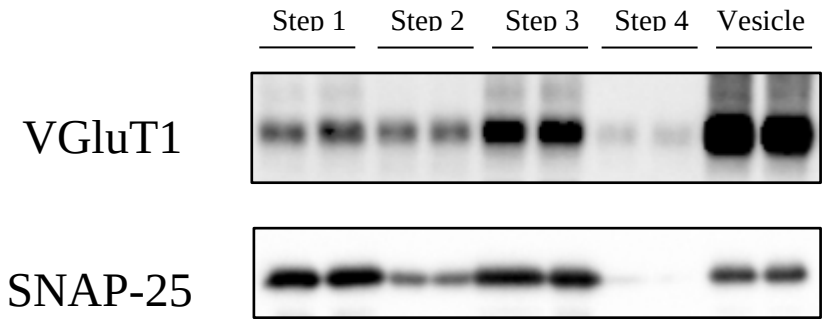

Figure 5. Isolation of crude vesicles. The vesicle pellets and the sample waste from each centrifuge step were collected and detected with vesicular protein anti-vGluT1 antibody and pre-synaptic protein anti-SNAP-25 antibody by western blot. Step 1-pellets from the 1st centrifuge; Step 2- supernatant from the 2nd centrifuge; Step 3-pellets from

the 3rd centrifuge; Step 4-supernatant from the 4th centrifuge; and Vesicle stands for isolated protein pellets from the 4th centrifuge.

2.5 Neurotransmitter Uptake Detection

Glutamate uptake was detected by incubating the aliquots of synaptic vesicles in the presence of different treatments in a final volume of 200 μl assay buffer containing 30 μg vesicle pellets, 10 mM K-HEPES (pH 7.4), 4 mM KCl, 4 mM MgSO4, 0.25 M sucrose and 2 mM L-aspartic acid (Asp) [147]. 2 mM ATP and 15 μM [^{3}H]glutamate were added into the 48-well plate to initiate the reaction since ATP is necessary for the uptake process. The final volumes were adjusted to 200 μl with assay buffer. Non-specific uptake was investigated by replacing ATP with equal volume of assay buffer [147]. The mixtures were incubated for 10 min at 37 °C, and then the reaction was terminated by quickly adding 1 ml ice-cold 150 mM KCl solution. Reaction solution from each system was suck to penetrate the filter paper, thus the vesicles would remain on the filter, while the solution containing unabsorbed radioisotope could pass the filter. The plate was then washed with 1 ml ice-cold 1 M KCl solution for 10 times. The filters containing [^{3}H]glutamate were transported to specific tubes and left overnight. Before testing, 5 ml of organic solvent (Ecolite) was added to the tubes. Radioactivity was counted by LS6000TA system (Beckman).

[^{3}H]Dopamine uptake was detected by incubating the aliquots of 30 μg synaptic vesicles in the assay buffer [pH 7.5] containing 25 mM HEPES, 100 mM potassium

tartrate, 50 μM EGTA, 100 μM EDTA 2 mM $MgSO_4$ and 17 mM ascorbic acid [146]. First, 2 mM ATP and 15 nM [^{3}H] dopamine was added into the 48-well plate to initiate the reaction. Non-specific uptake was investigated by switching ATP with equal volume of assay buffer [146]. The final volumes were adjusted to 200 μl with assay buffer, and then incubated at 37 °C for 10 min. The reaction was terminated by quickly adding 1 ml of ice-cold assay buffer. The plate was then washed with 1 ml assay buffer for 10 times. The filters containing [^{3}H]dopamine were left overnight. Radioactivity of dopamine was counted by LS6000TA system (Beckman).

[^{3}H] Acetylcholine uptake was detected by incubating the aliquots of 30 μg synaptic vesicles at 37 °C for 10 min in the assay buffer in the assay buffer [pH 7.5] containing 25 mM HEPES, 100 mM potassium tartrate, 50 μM EGTA, 100 μM EDTA, 2 mM $MgSO_4$ and 17 mM ascorbic acid. A final concentration of 50 μM paraoxon was used as cholinesterase inhibitor to inhibit the degradation of acetylcholine by cholinesterase [148]. The mixture 2 mM ATP and 150 nM [^{3}H]acetylcholine was added into the 48-well plate to initiate the reaction. Non-specific reaction was investigated by replacing ATP with assay buffer. The final volumes were adjusted to 200 μl, and then incubated in 37 °C water bath for 10 min. After incubation, 1 ml ice-cold assay buffer was quickly added to each well to terminate the reaction, followed by 10 times washing with assay buffer (1 ml per time) [148]. The filters containing [^{3}H]acetylcholine were

left overnight. Radioactivity of acetylcholine was counted by LS6000TA system (Beckman).

2.6 Biotin-Switch Assay for Detection of S-Nitrosylated Proteins

For the total protein S-nitrosylation detection, 50 μl of tissue extracts (1.0 μg/μl) from wild type mouse brain or APP/PS1 mouse brain was added with 200 μl of blocking buffer [2.5% SDS, 40 mM N-ethylmaleimide [NEM] in HEN buffer (250 mM Hepes-NaOH pH 7.7, 1 mM EDTA, 0.1 mM neocuproine)] and incubated for 40 min at 50 °C to block free thiol groups. After the samples were blocked, 1 ml cold 99% acetone was added to each sample. Then the samples were precipitated at -20 °C for 15 minutes. After the samples were centrifuged, the supernatant containing excess NEM was removed, and the pellets were resolved with 10 μl HENS buffer (250 mM Hepes-NaOH pH 7.7, 1 mM EDTA, 1% SDS, 0.1 mM neocuproine), followed by reduction of S-nitrosothiols (-SNO) with 250 μl of 1 mM ascorbate. The newly formed free thiols were labelled with 15 μl of 4 mM *N*-[6-(biotinamido)hexyl]-3'-(2'-pyridyldithio) propionamide (Biotin-HPDP) [149,150]. 10 μl of total reaction system (S-nitrosylated protein) from each sample was detected with anti-biotin antibody by immunoblotting.

For individual protein S-nitrosylation, the biotinylated proteins obtained were precipitated with 1 ml cold 99% acetone. After the samples were centrifuged, the pellets

were resolved with 10 µl HENS buffer. Then 5 µl of streptavidin-agarose beads, which have specific affinity for biotin, was added to each sample and incubated for 1 h at room temperature to precipitate biotinylated proteins. The samples were washed with 300 µl of washing buffer **(**Hepes-NaOH pH 7.7, 20 mM, NaCl 600 mM, EDTA 1 mM, Triton X-100 0.5%) for five times and eluted with 100 µl of elution buffer (Hepes-NaOH, pH 7.7 20 mM, NaCl 100 mM, EDTA 1 mM, 2-ME 100 mM) [149,150]. Immunoblotting was performed to detect the amount of different vesicular transporters remaining in the samples with specific antibodies for these transporters.

2.7 Immunoblotting Analysis

For measuring expression of transporters, 10 µg of each brain extract was loaded into each lane of the 10% sodium dodecyl sulphate polyacrylamide gel (SDS-PAGE) for electrophoresis, while for measuring S-nitrosylated protein after biotin switch method, 10 µl of each sample system was loaded. Gels were run at 80 V for first 20 min and then 120 V for approximately 1 h. The proteins on the gels were then transferred to PVDF membranes at 220 mA for 2 h. Membranes were first blocked with 5% (w/v) milk in TBST buffer (10 mM Tris-HCl, pH 7.5, 0.1% Tween-20) for 1 hour at room temperature and then incubated with various primary antibodies for 16 h at 4°C. The concentrations of different antibodies were as follow: anti-biotin antibody (1:3000, Sigma), anti-vGluT1 antibody (1:1500, Abcam), anti-vGluT2 antibody (1:1000, Millipore),

anti-vMAT2 (1:1000, Abcam), anti-vAChT antibody (1:1000, Abcam), Anti-SNAP 25 antibody (1:100). The concentrations of secondary antibodies were as follows: goat anti-rabbit (1:7000, Jackson & Immuno Research) or goat anti-mouse (1:8000, Abcam). After primary and second antibody incubation, the membranes were washed with TBST buffer for 15 min three times. The membranes were developed using electrochemiluminescence (ECL) reagents (PerkinElmer) in the ChemiDoc MP System (Bio-Rad). Band signal intensity was quantified by measuring the density of the band using Image Lab (Bio-Rad).

2.8 Statistical Analysis

Statistical analysis was performed using the SPSS13.0 software. All the results were expressed as means ± SE. Statistical significance of differences among means was determined by analysis of variance (one-way ANOVA) with *Turkey post hoc* comparison using SPSS13.0 software. Student's *t*-tests were also performed for statistical analysis of two groups comparison. A *p* value of less than 0.05 was regarded as statistically significant.

CHAPTER 3: RESULTS

3.1 To investigate whether vesicular neurotransmitter transporters can be S-nitrosylated

3.1.1 NO• radicals can induce S-nitrosylation of vAChT, vMAT2, vGluT1 and vGluT2

First, we verified the methodology of biotin switch method. 50 µg homogenate of mouse brain was used for each reaction. Ascorbate (reducing agent) and biotin-HPDP (labeling agent) was missing in different reaction to check the false positive signal, and 20 µM GSNO (NO donor) was added to see the global access of free thiol groups within the proteins. As show in Figure 6, lane 1 and lane 2 demonstrate very small positive signal compared to control group (lane 3), which were caused by incomplete blocking and endogenous biotinylation. Lane 4 demonstrated a much more intensive signals than control group.

Second, we analyzed if GSNO can increase total protein S-nitrosylation using the biotin switch method. GSNO at 20, 40 or 80 µM was incubated with 50 µg homogenate of mouse brain for 30 min at room temperature. As shown in Figure 7, significant difference of cysteine S-nitrosylation was detected in all GSNO treatment groups ($F_{(5,18)} = 61.944$, $p = 0.000$) and S-nitrosylation was increased dose-dependently by GSNO. The result indicated that free cysteine thiols in proteins are accessible for NO, and can be S-nitrosylated by GSNO.

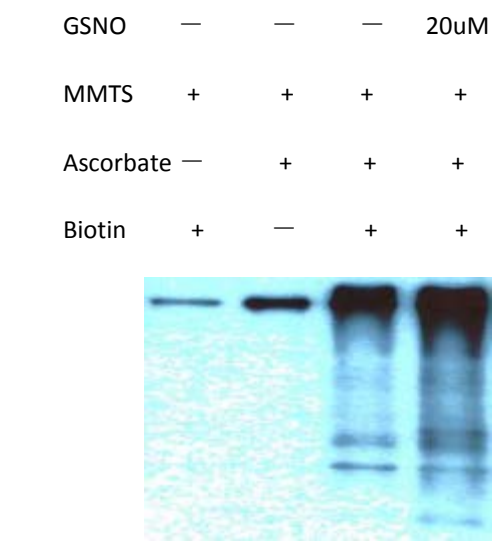

Figure 6. Biotin switch methodology. The protein samples were treated with or without GSNO, and then blocked with or without NEM, followed by reduction with or without ascorbate. Biotin-HPDP was used to label reduced free thiols. Immunoblotting was employed to check total S-nitrosylation with anti-biotin antibody. For the methodology, lane 1 shows S-nitrosylated proteins in the samples without ascorbate; lane 2 shows signal intensity of S-nitrosylated proteins in the absence of biotin-HPDP; lane 3 shows the amount of S-nitrosylated cysteines in the sample; and lane 4 shows an increased intensity of biotin signal with 20 μM GSNO treatment.

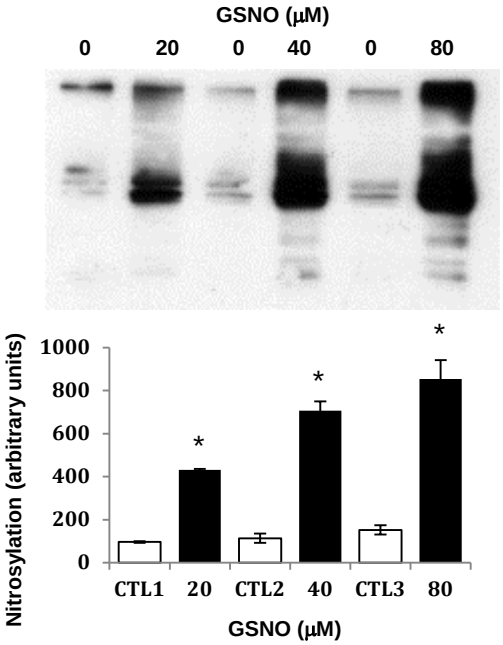

Figure 7. GSNO increased total cysteine S-nitrosylation. Mouse brain lysate was prepared in dark room to protect the nitrosothiol groups, and lysate was adjusted to 1.0 µg/µl. Biotin-Switch method was performed to check the S-nitrosylated thiol groups in the samples. Equal volumes of lysates with a total of 50 µg protein from mouse brain were processed as indicated for different treatments, and then western blot was performed to check the biotin signal. Concentration response was investigated by applying different concentrations of GSNO to treat the samples. Data are displayed as mean ± SEM (n = 4). * indicates $p < 0.05$ by one-way ANOVA, *Turkey's post hoc* test.

Third, to investigate whether vesicular transporters can be S-nitrosylated, the effect of GSNO on thiol S-nitrosylation of vGluT1, vGluT2, vMAT2 and vAChT was measured. GSNO at 40, 80 and 160 µM was incubated with 50 µg homogenate of mouse brain for 30 min at room temperature. In this experiment, biotinylated proteins (S-nitrosylated) were precipitated by streptavidin-agarose beads and the precipitated proteins were analysed by a specific antibody for vGluT1, vGluT2, vMAT2 and vAChT respectively. As shown in Figure 8A, one-way ANOVA test reveals a significant difference of vAChT S-nitrosylation among treatment groups ($F_{(3,12)} = 9.715$, $p = 0.001$). Although GSNO at 40 µM has no effect on vAChT nitrosylation, GSNO at 80 and 160 µM significantly increased vAChT S-nitrosylation by 102 ± 3% ($p < 0.05$) and 254 ± 63% ($p < 0.05$) respectively.

Figure 8B shows the result of GSNO on vMAT2 S-nitrosylation. One-way ANOVA test demonstrated a significant difference of vMAT S-nitrosylation among GSNO treatment groups ($F_{(3,12)} = 6.690$, $p = 0.002$). GSNO at 40 µM, at 80 µM and 160 µM increased vMAT S-nitrosylation by 80 ± 20%, 260 ± 43% and 340 ± 103%

respectively. Within these treatments, 80 µM and 160 µM GSNO showed a significant increase of vMAT2 S-nitrosylation ($p < 0.05$). This result suggests that free cysteine thiols in vMAT2 can be attacked by NO radicals. vGluT1 and vGluT2 are two main isoforms of vesicular glutamate transporters in different areas of the brain, in which vGluT1 predominates in hippocampus and cerebral cortices, whereas vGluT2 expression is prominent in brainstem, diencephalon and spinal cord [151,152,153]. In Figure 8C, a significant difference of vGluT1 S-nitrosylation could be detected by one-way ANOVA ($F_{(3,12)} = 16.800$, $p = 0.000$). In detail, GSNO increased S-nitrosylation of vGluT1 by 22 ± 6% at 40 µM, 70 ± 8% at 80 µM and 120 ± 13.7% at 160 µM. GSNO at 40 µM has no effect on the S-nitrosylation of vGluT1, but GSNO at 80 µM and 160 µM significantly increased the S-nitrosylation of vGluT1 ($p < 0.05$). In Figure 8D, significant difference was detected on the S-nitrosylation of vGluT2 by different GSNO treatments ($F_{(3,12)} = 21.845$, $p = 0.000$). S-nitrosylation of vGluT2 was increased by 64 ± 9% at 40 µM, 162 ± 17% at 80 µM and 184 ± 21% at 160 µM. Statistical significance was detected at 40 µM, 80 µM and 160 µM GSNO treatments ($p < 0.05$), indicating that vGluTs could also be the targets for NO and NO donors within the cells.

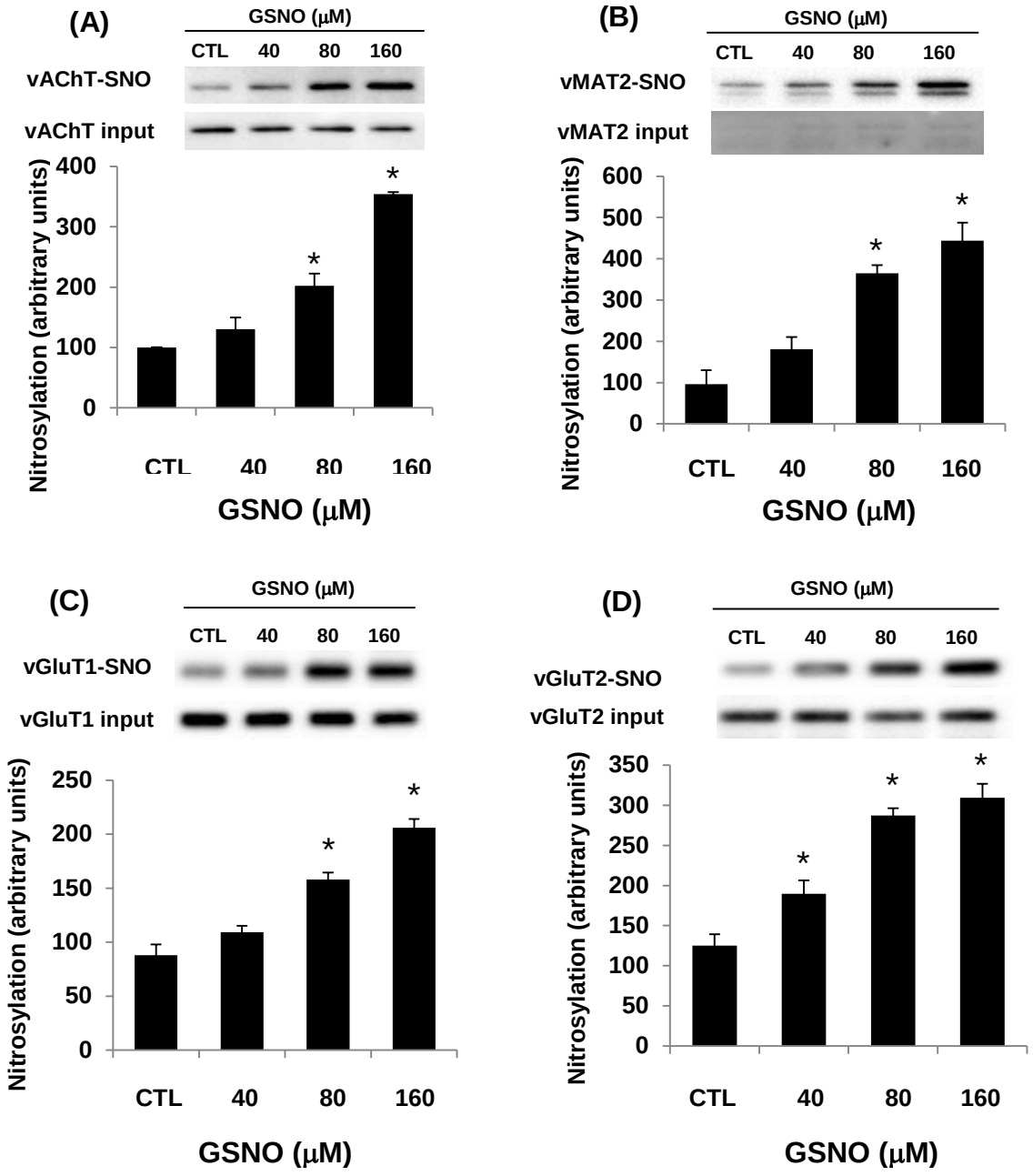

Figure 8. NO• donor S-nitrosoglutathione (GSNO) increased S-nitrosylation of vesicular acetylcholine transporter (vAChT), vesicular monoamine transporter 2 (vMAT2), vesicular glutamate transporter type 1 (vGluT1) and type 2 (vGluT2). Protein isolated from mouse brain was treated with GSNO at 40, 80 and 160 μM for 30 min. A control group was set in the first lane of each reaction in which no GSNO was added to show the basal S-nitrosylation of vAChT (A), vMAT2 (B), vGluT1 (C) or vGluT2 (D) and the trace amount of each vesicular transporter remaining after washing.

Protein input was detected in a separate gel, which can be used as equal loading. Free thiols were blocked with NEM, and then protein S-nitrosylation were reduced by ascorbate and labeled with biotin-HPDP. Biotinylated proteins were precipitated by avidin agarose. S-nitrosylated vAChT (A), vMAT2 (B), vGluT1 (C), and vGluT2 (D), (vAChT-SNO, vMAT2-SNO, vGluT1-SNO and vGluT2-SNO), were analyzed by immunoblotting with anti-vAChT, anti-vMAT2, anti-vGluT1 and anti-vGluT2 antibodies respectively. Data are displayed as mean ± SEM (n = 4). * indicates $p < 0.05$ by one-way ANOVA followed by *Turkey's post hoc* test.

3.1.2 NO• donor S-nitrosoglutathione (GSNO) inhibits uptake of glutamate, acetylcholine and dopamine by synaptic vesicles

Vesicular neurotransmitter transporters mediate the uptake of various neurotransmitters into synaptic vesicles. S-nitrosylation of vesicular transporters may have a high impact on the uptake of neurotransmitters [134,154]. Therefore we analyzed the effect of NO• donor GSNO on vesicular uptake of [^{3}H]glutamate, [^{3}H]acetylcholine and [^{3}H]dopamine.

First, we investigated whether uptake of [^{3}H]glutamate, [^{3}H]acetylcholine and [^{3}H]dopamine by isolated vesicles is mediated by different vesicular neurotransmitter transporters. We analyzed the effect of rose bengal (vGluTs inhibitor), vesamicol (vAChT inhibitor) and reserpine (vMATs inhibitor) on vesicular uptake of [^{3}H]glutamate, [^{3}H]acetylcholine and [^{3}H]dopamine. All of these inhibitors were added to the vesicles before the reaction was initiated (before ATP and radioisotope were added to the samples). As shown in Figure 9A-C, after non-specific values were subtracted from each group, 20 µM rose bengal significantly inhibited the uptake of

[^{3}H]glutamate (100 ± 18% vs 2 ± 9%, t_{10} = 5.132, $p < 0.05$); 40 μM vesamicol inhibited the uptake of [^{3}H]acetylcholine, which is not significant (100 ± 38% vs 51 ± 24%, t_{10} = 1.371, $p = 0.213$); and 20 μM reserpine significantly inhibited the uptake of [^{3}H]dopamine (100 ± 8% vs 5 ± 12%, t_{10} = 8.465, $p < 0.05$).

Second, the effect of GSNO on vesicular uptake of neurotransmitters was analyzed. The vesicles were treated with 40, 80 and 160 μM GSNO for 30 min at room temperature, which was exactly same as the *in vitro* S-nitrosylation study, followed by neurotransmitter uptake detection. As shown in Figure 10A, GSNO at 40-160 μM concentration-dependently decreased vesicular uptake of [^{3}H]glutamate ($F_{(3,20)}$ = 32.822, $p = 0.000$). GSNO at 80 μM significantly decreased vesicular uptake of [^{3}H]glutamate to 42 ± 8% ($p < 0.05$); GSNO at 160 μM also significantly decreased vesicular uptake of [^{3}H]glutamate to -2 ± 3% ($p < 0.05$) when compared to control group. Although GSNO at 40 μM decreased [^{3}H]glutamate, this decrease does not show any statistical significance. GSNO at 40-160 μM also concentration-dependently decreased vesicular uptake of [^{3}H]acetylcholine ($F_{(3,20)}$ = 9.160, $p = 0.001$)(Fig 10B). GSNO at 40, 80 and 160 μM significantly decreased vesicular uptake of [^{3}H]acetylcholine to 36 ± 8% ($p < 0.05$); 15 ± 5% ($p < 0.05$) and 6 ± 5% ($p < 0.05$) respectively. GSNO at 40-160 μM also concentration-dependently decreased vesicular uptake of [^{3}H]dopamine ($F_{(3,20)}$ = 9.160, $p = 0.001$)(Fig 10C). GSNO at 160 μM significantly decreased vesicular uptake of

[^{3}H]dopamine to 54 ± 4% ($p < 0.05$). Although GSNO at 40 µM and 80 µM also decreased [^{3}H]dopamine, this decrease does not show any statistical significance.

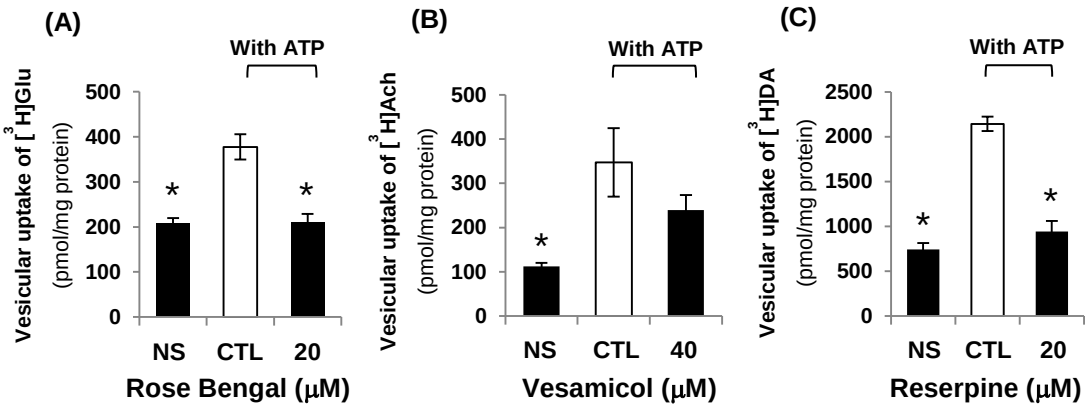

Figure 9. Specificity of vesicular glutamate, acetylcholine and dopamine uptake. (A)(B) and (C) Vesicles were treated with vehicle (CTL), vGluT inhibitor rose bengal at 20 µM or vAChT inhibitor vesamicol at 40 µm or vMAT2 inhibitor reserpine at 20 µM, then [^{3}H]glutamate uptake or [^{3}H]acetylcholine or [^{3}H]dopamine uptake was detected under ATP. [^{3}H]Glutamate or [^{3}H]acetylcholine or [^{3}H]dopamine uptake without ATP was used as non-specific (NS) uptake. Data are presented as the mean ± SEM (n = 6). * indicates $p < 0.05$ when compared to controls determined by Student's *t* test.

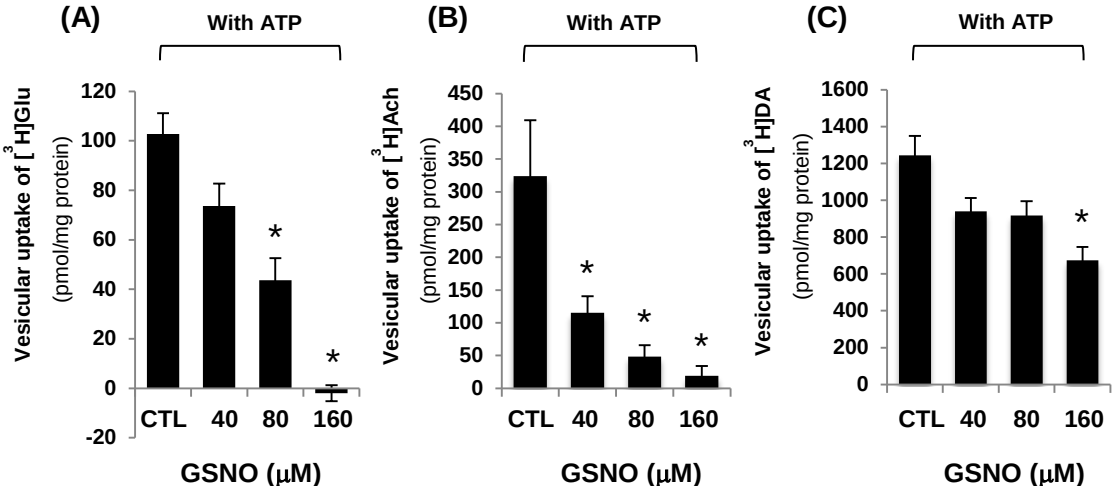

Figure 10. NO• donor S-nitrosoglutathione (GSNO) inhibits vesicular glutamate, acetylcholine and dopamine uptake. (A) (B) and (C) Vesicles were treated with GSNO at 40 - 160µM GSNO, then [^{3}H]glutamate uptake, ^{3}[H]acetylcholine uptake or [^{3}H]dopamine uptake was detected under ATP. Results of CTL and GSNO treatment groups from different studies are presented by subtracting NS uptake values. Data are presented as the mean ± SEM (n = 6). * indicates $p < 0.05$ when compared to controls determined by one-way ANOVA by *post hoc Turkey* test.

3.2 To investigate short-term memory and spatial memory in APP/PS1 mouse model

3.2.1 Short-term memory is damaged in early stage of APP/PS1 Mice

Four age-groups (3, 6, 9 and 12 months) of APP/PS1 mice and same-age wild-type mice were used for our studies. Because any deficits of locomotion in animal may affect memory tests, we first measured locomotor activity using open field test in wild-type and APP/PS1 mice. As shown in Figure 11A, no significant difference was detected in terms of locomotor activity between APP/PS1 mice and wild type mice in each age group by Student' *t*-test. This result suggests that the APP/PS1 double transgenic mice used in the study does not display any locomotor deficit when compared to wild type mice.

Next the short-term memory was analyzed using Y Maze spontaneous alternation test. As shown in Figure 11B, the percentage of correct triads in 3 month old APP/PS1 mice is significantly lower than in the same age wild type control mice (61.7 ± 3.3% vs 73.9 ± 2.2%, $p < 0.05$). However the percentage of correct triads is not significant different between 6 month old APP/PS1 mice and their controls (63.0 ± 3.4% vs 69.3 ± 3.7%, $p = 0.284$); between 9 month old APP/PS1 mice and their controls (65.3 ± 4.4% vs 67.4 ± 1.9%, $p = 0.668$); or between 12 month-old APP/PS1 mice and their controls (64.5 ± 2.5% vs 66.3 ± 4.0%, $p = 0.744$). The result indicates that short-term memory

loss could only be detected at early age of $APP_{K670N/M671L}/PS1_{M146L}$ transgenic animal model.

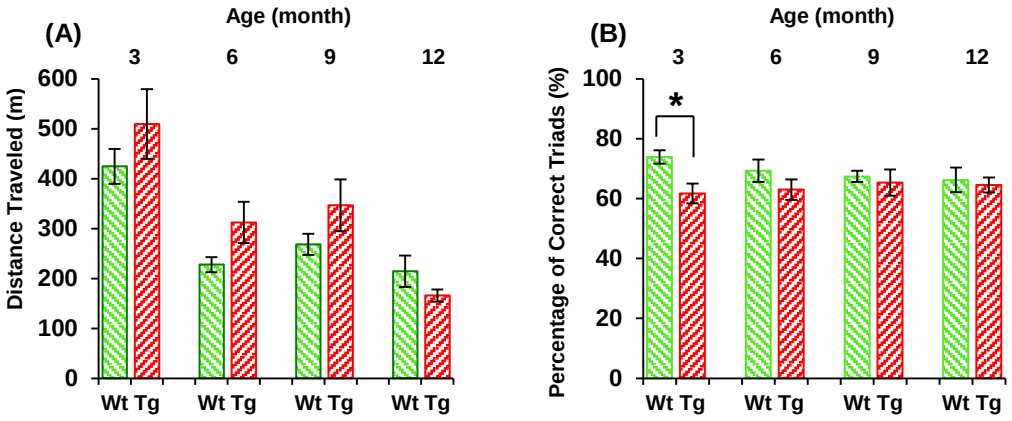

Figure 11. Short term memory is damaged in 3 month APP/PS1 transgenic (Tg) mice. (A) The average distance moved for 1 h in the open field of 3, 6, 9 and 12 month APP/PS1 (Tg) and wild type mice (WT). The distance moved for each mouse was recorded and analyzed with EthoVision XT system. No statistically significant difference was detected between APP/PS1 and wild type mice within each group. (B) The average percentage of right triads plotted in Y maze test of 3, 6, 9 and 12 month APP/PS1 (Tg) and wild type mice (WT) with EthoVision XT system. The Tg and WT mice were put in the Y maze to freely explore the three arms for 8 min. The entry sequence was recorded and analyzed for short-term memory. Data are displayed as mean ± SEM. 3 month: Tg = 10, WT = 9; 6 month: Tg = 6, WT = 10; 9 month: Tg = 9, WT = 9; 12 month: Tg = 5, WT = 9. * indicates $p < 0.05$ by Student's *t* test.

3.2.2 Acquisition of spatial reference memory is impaired in 9 and 12 month APP/PS1 double transgenic mice.

Having established that no hyperactivity was found between the APP/PS1 and wild type mice based on previous open field test, MWM was performed to examine the recall and spatial memory. First, the swimming speed and swimming distance were investigated to

show the physiological conditions of the mice during the test. As illustrated in Figure 12A and B, no significant difference was detected between APP/PS1 mice and their wild type littermates in terms of swimming speed and swimming distance in each age group by Student' *t*-test. These results indicate no hyperactive or hypoactive physiological conditions during the test between groups.

Second, latency and crossing numbers in MWM were detected to show the spatial memory loss in APP/PS1 mice. In Figure 12C, the escape latency was not significantly different between the 3 month APP/PS1 mice and their wild type littermates (15.3 ± 3.5 s vs 13.9 ± 5.2 s, $t_{17} = -0.210$, $p = 0.836$); or between the 6 month APP/PS1 mice and their wide type littermates (19.8 ± 5.8 s vs 11.8 ± 2.2 s, $t_{14} = -1.529$, $p = 0.148$). The escape latency was significantly longer in the 9 month APP/PS1 double transgenic mice than that in their wild type littermates (26.6 ± 7.3 vs 10.1 ± 2.8, $t_{16} = -3.079$, $p < 0.05$); and significantly longer in the 12 month APP/PS1 mice than in their wild type littermates (44.8 ± 9.1 vs 15.1 ± 2.7, $t_{12} = -4.816$, $p < 0.05$). These results suggest that the APP/PS1 double transgenic mice show a clear impairment in acquisition of the MWM in 9 month and 12 month APP/PS1 mice.

In addition to escape latency, the number of crossings was also recorded. In Figure 12D, the number of crossings was not significantly different between the 3 month APP/PS1 mice and their wild type littermates (2.3 ± 0.5 vs 3.3 ± 0.5, $t_{17} = 0.873$, $p = 0.080$); or between the 6 month APP/PS1 mice and the wild type mice (3.0 ± 0.5 vs 2.9

± 0.3, t_{14} = -0.167, p = 0.870). However, the crossing numbers are significantly decreased in the 9 month APP/PS1 mice when compared to their wild type mice (2.4 ± 0.7 vs 3.6 ± 0.5, t_{16} = 1.964, $p < 0.05$); and in the 12 month APP/PS1 when compared to their wild type littermates (0.5 ± 0.2 vs 2.5 ± 0.3, t_{12} = 3.453, $p < 0.05$). The result indicates a damage of spatial memory accuracy in 9 and 12 month APP/PS1 double transgenic mice.

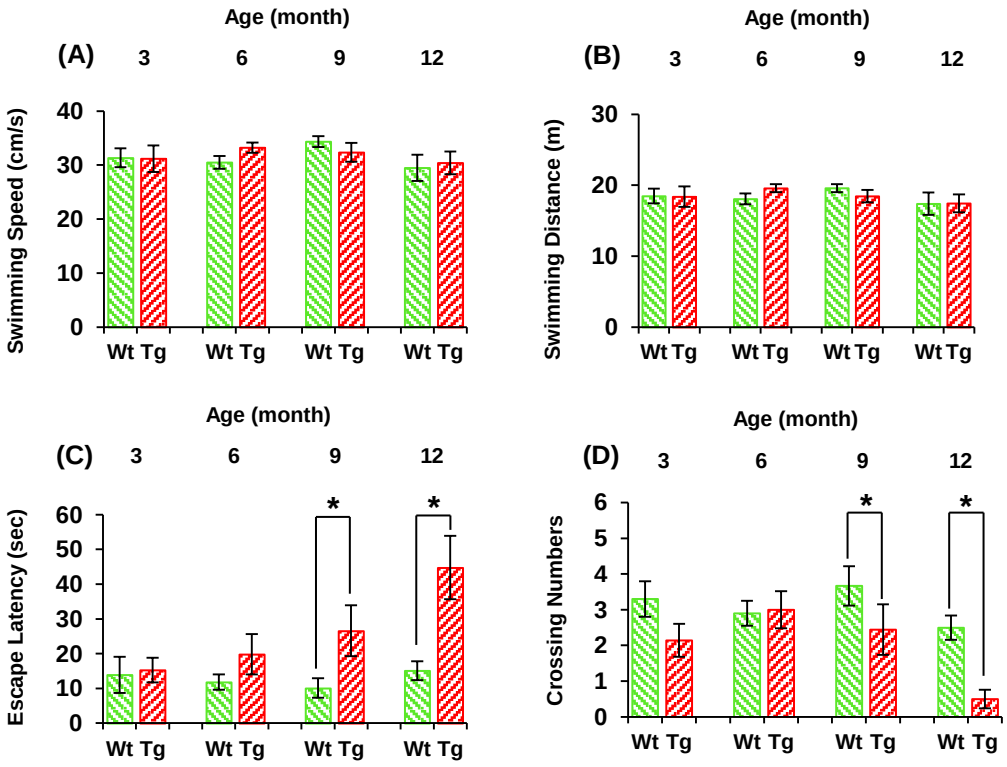

Figure 12. Acquisition of spatial memory is impaired in 9 and 12 month APP/PS1 Transgenic (Tg) mice. The average swimming speed (A) and the average swimming distance (B) of all the mice were detected during the probe trial. There is no significant difference between the APP/PS1 Transgenic (Tg) mice and the Wild Type (WT) mice within each age group. (C) The escape latency of the mice during the probe trial on day 5 of the APP/PS1 mice and the wild type mice of all ages during MWM. (D) The number of crossings through platform area during the probe trial on day 5 for the transgenic mice and the wild type mice for all age groups. Data are displayed as mean ±

SEM, 3 month: Tg = 10, WT = 9; 6 month: Tg = 6, WT = 10; 9 month: Tg = 9, WT = 9; 12 month: Tg = 5, WT = 9. * indicates $p < 0.05$ by Student's *t* test.

3.3 To investigate total protein S-nitrosylation of frontal cortex and hippocampus from wild type mice and APP/PS1 double transgenic mice

In this section, we investigated the changes of total protein S-nitrosylation in the frontal cortex and hippocampus extracts from all age groups respectively. According to statistic result in Figure 13A, no significant difference in terms of total protein S-nitrosylation was detected between 3 month APP/PS1 mice and their wild type mice (0.99 ± 0.13 vs 1.10 ± 0.07, $t_{17} = 0.687$, $p = 0.489$); or between the 6 month APP/PS1 mice and the wild type mice (1.27 ± 0.18 vs 1.30 ± 0.10, $t_{14} = 0.170$, $p = 0.867$). Interestingly, significant increase of total protein S-nitrosyaltion was detected in the 9 month APP/PS1 mice compared to their wide type littermates (1.27 ± 0.10 vs 0.87 ± 0.12, $t_{16} = -2.163$, $p < 0.05$); and in the 12 month APP/PS1 compared to their wild type littermates (1.45 ± 0.17 vs 0.59 ± 0.04, $t_{12} = -6.402$, $p < 0.05$).

In Figure 13B, total protein S-nitrosyaltion in the hippocampus extracts was not significantly different between the 3 month APP/PS1 mice and their wild type littermates (0.98 ± 0.05 vs 1.12 ± 0.07, $t_{17} = 1.632$, $p = 0.121$); or between the 6 month APP/PS1 mice and their wild type littermates (1.18 ± 0.08 vs 1.16 ± 0.10, $t_{14} = -0.115$, $p = 0.910$). However, total protein S-nitrosyaltion in the hippocampus extracts was significant higher in 9 month APP/PS1 mice than that in their wild type littermates (1.21

± 0.10 vs 0.92 ± 0.07, $t_{16} = -2.374$, $p < 0.05$); and significantly higher in the 12 month APP/PS1 mice than that in their wild type littermates (1.16 ± 0.07 vs 0.90 ± 0.05, $t_{12} = -3.227$, $p < 0.05$).

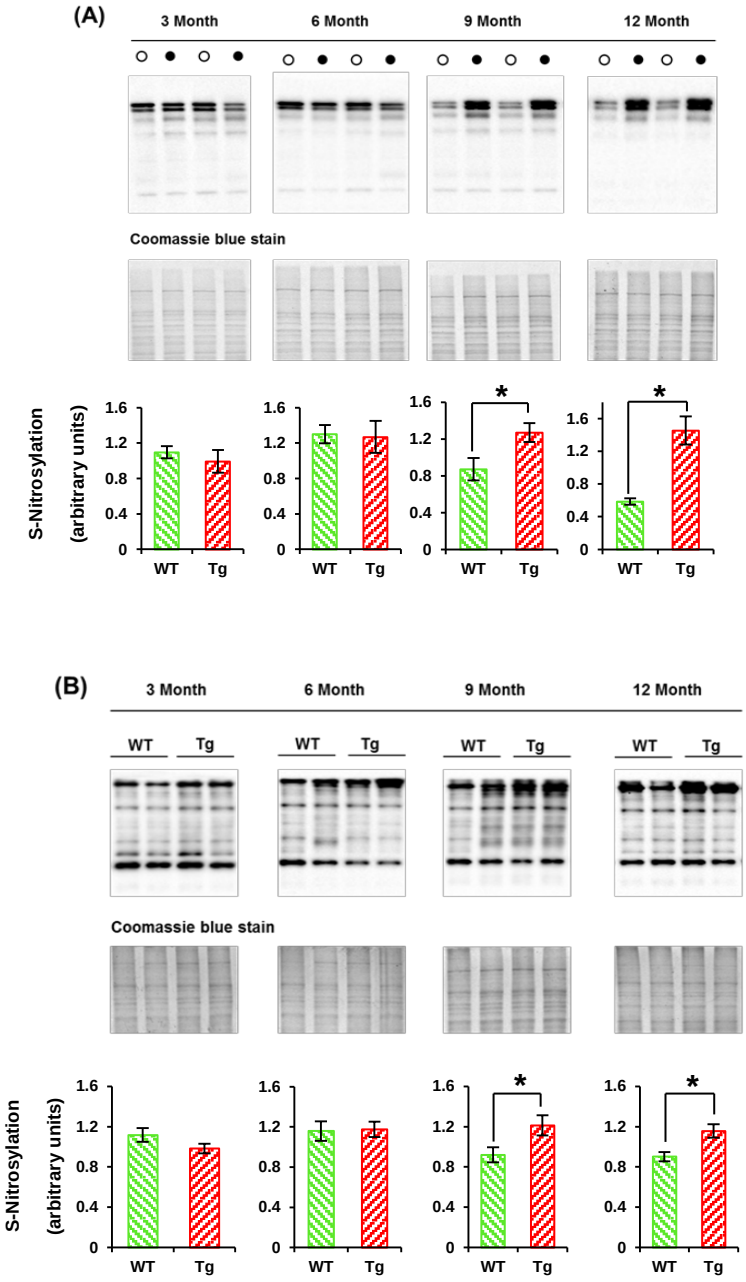

Figure 13. Total protein S-nitrosylation of frontal cortex and hippocampus from Wild Type (WT) mice and APP/PS1 Transgenic (Tg) Mice. Frontal cortex (A) and

hippocampus (B) were isolated and lysed respectively, followed by biotin switch method. Immunoblotting was performed to check the biotin signal with anti-biotin antibody. (A) Black circles stand for APP/PS1 (Tg) mice and white circles stand for wild type (WT) mice. Membranes after immunoblotting from A and B were washed and stained with coomassie blue to check equal loading of each lane. Data are displayed as mean ± SEM, 3 month: Tg = 10, WT = 9; 6 month: Tg = 6, WT = 10; 9 month: Tg = 9, WT = 9; 12 month: Tg = 5, WT = 9. * indicates $p < 0.05$ by Student's *t* test.

3.4 To investigate S-nitrosylation of vGluT1 and vAChT in frontal cortex and hippocampus

3.4.1 vGluT1 and vAChT S-nitrosylation are increased in frontal cortex and hippocampus from APP/PS1 transgenic Mice.

Previously we have found that vesicular neurotransmitter transporters can be S-nitrosylated, therefore we investigated S-nitrosylation of these transporters in frontal cortex and hippocampus extracts of APP/PS1 and wild type mice in 4 age groups. vGluT1 S-nitrosylation and vAChT S-nitrosylation were increased in frontal cortex extracts from different age groups of the mice (Fig 14A). In all frontal cortex samples, no significant difference was detected in terms of vGluT1 S-nitrosylation between the 3 month APP/PS1 mice and their wild type littermates (1.09 ± 0.03 vs 0.93 ± 0.07, $t_{17} = -1.735$, $p = 0.113$). Interestingly, significant increase of vGluT1 S-nitrosylation was detected in the 6 month APP/PS1 mice compared to their wild type mice (1.38 ± 0.12 vs 0.99 ± 0.04, $t_{14} = -3.768$, $p < 0.05$); in the 9 month APP/PS1 mice compared to their wild type littermates (1.15 ± 0.08 vs 0.88 ± 0.06, $t_{16} = -2.780$, $p < 0.05$); and in the 12

month APP/PS1 mice compared to their wild type littermates (2.35 ± 0.51 vs 0.89 ± 0.01, $t_{12} = -2.779$, $p < 0.05$). The vAChT S-nitrosylation in frontal cortex extracts from all age groups shared the same pattern as vGluT1 S-nitrosylation. According to the result in Figure 14B, no significant difference was detected in terms of vAChT S-nitrosylation between the 3 month APP/PS1 mice and their wild type littermates (1.40 ± 0.22 vs 1.03 ± 0.20, $t_{17} = -1.253$, $p = 0.227$). However, significant increase of vAChT S-nitrosylation was detected in the 6 month APP/PS1 mice compared to their wild type mice (2.51 ± 0.47 vs 0.76 ± 0.10, $t_{14} = -3.660$, $p < 0.05$); in the 9 month APP/PS1 mice compared to their wild type mice (1.87 ± 0.23 vs 0.70 ± 0.12, $t_{16} = -5.268$, $p < 0.05$); and in the 12 month APP/PS1 mice compared to their wild type mice (8.31 ± 2.52 vs 0.83 ± 0.15, $t_{12} = -2.958$, $p < 0.05$). Significant increase of vGluT1 S-nitrosylation and vAChT S-nitrosylation in hippocampus extracts from 6, 9 and 12 month APP/PS1 mice indicates that vAChT could be S-nitrosylated caused by Aβ toxicity.

We continued to investigate vGluT1 S-nitrosylation and vAChT S-nitrosylation in hippocampus extracts from all age groups. In Figure 15A, significant increase of vGluT1 S-nitrosylation was detected in the 3 month APP/PS1 mice compared to their wild type littermates (1.62 ± 0.23 vs 0.77 ± 0.08, $t_{17} = -4.149$, $p < 0.05$). However, no significant difference of vGluT1 S-nitrosylation was detected between the 6 month APP/PS1 mice and their wild type littermates (1.03 ± 0.05 vs 1.03 ± 0.08, $t_{14} = -0.017$, $p = 0.986$); between the 9 month APP/PS1 mice and their wild type littermates (0.92 ± 0.04 vs 1.07

± 0.12, $t_{16} = 1.253$, $p = 0.239$); or between the 12 month APP/PS1 mice and their wild type littermates (1.04 ± 0.15 vs 1.07 ± 0.14, $t_{12} = 0.121$, $p = 0.906$). In Figure 15B, significant increase of vAChT S-nitrosylation was detected in the 3 month APP/PS1 mice compared to their wild type littermates (1.64 ± 0.19 vs 0.73 ± 0.13, $t_{17} = -3.886$, $p < 0.05$), indicating that S-nitrosylation of vAChT is an early onset event in hippocampus. However, no significant difference of vAChT S-nitrosylation was detected between the 6 month APP/PS1 mice and their wild type littermates (1.07 ± 0.11 vs 0.97 ± 0.13, $t_{14} = -0.525$, $p = 0.607$); between the 9 month APP/PS1 mice and their wild type littermates (1.18 ± 0.20 vs 0.93 ± 0.22, $t_{15} = -0.859$, $p = 0.404$); or between the 12 month APP/PS1 mice and their wild type littermates (0.61 ± 0.13 vs 0.73 ± 0.15, $t_{12} = 0.543$, $p = 0.598$). This result indicates an early onset event of vGluT1 S-nitrosylation and vAChT S-nitrosylation in the hippocampus from the APP/PS1 mice.

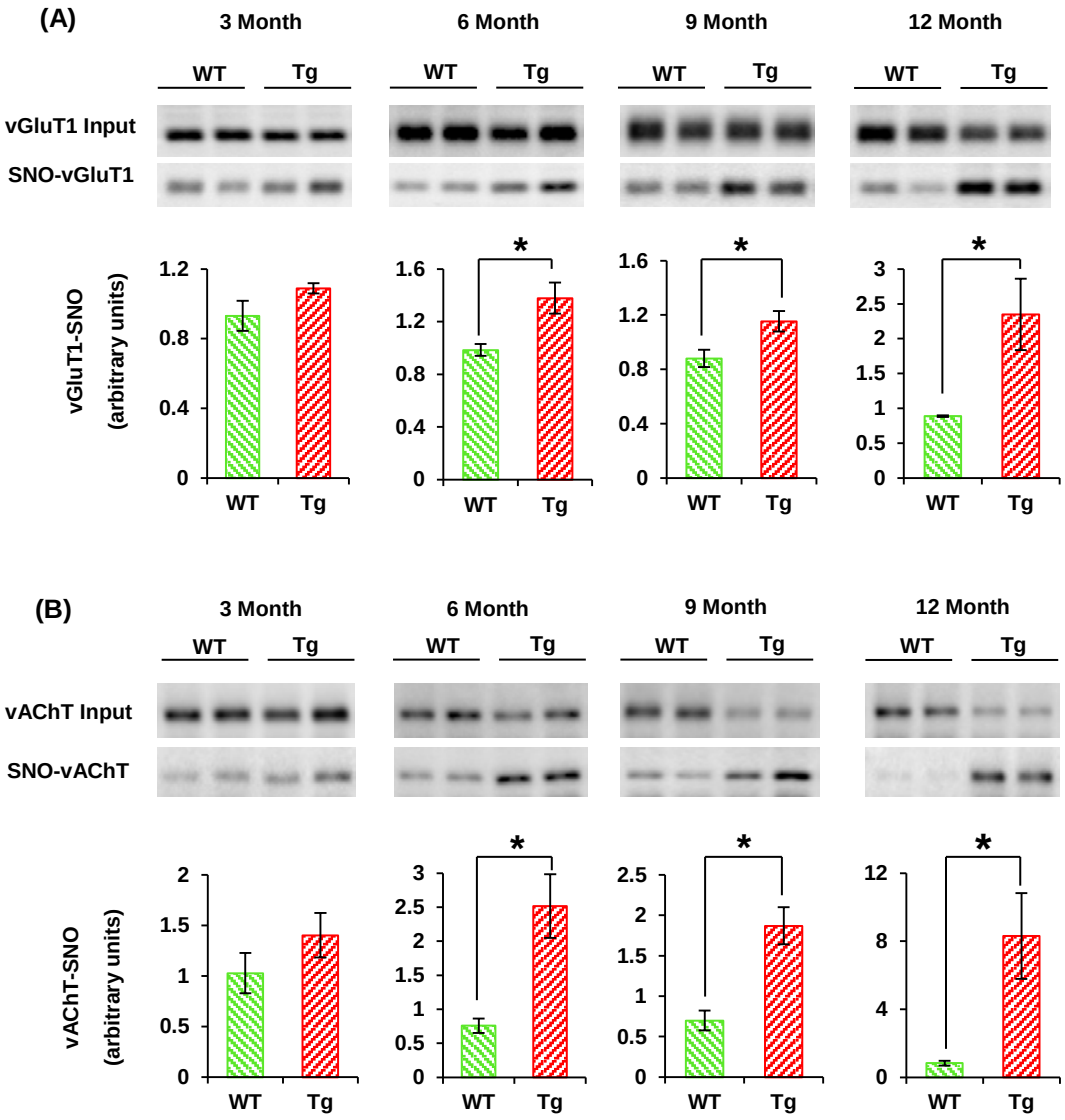

Figure 14. vGluT1 and vAChT S-nitrosylationin frontal cortex from Wild Type (WT) mice and APP/PS1 Transgenic (Tg) Mice. vGluT1 S-nitrosylation (vGluT1-SNO) (A) and vAChT S-nitrosylation (vAChT-SNO) (B) were investigated in the frontal cortex extracts from all age groups of APP/PS1 and wild type mice. Biotin switch method was employed to switch S-nitrosylated cysteines with biotin. Biotinylated proteins were then precipitated by avidin agarose. Immunoblotting was performed to check the vGluT1 (A) and vAChT (B) with anti-vGluT1 and anti-vAChT antibody. vGluT1 input (A) and vAChT input (B) were used to check the protein equal loading respectively, in which a small amount of samples were separated before precipitation, and then loaded in a separate gel. Data are displayed as mean ± SEM, 3 month: Tg = 10, WT = 9; 6 month: Tg = 6, WT = 10; 9 month: Tg = 9, WT = 9; 12 month: Tg = 5, WT = 9. * indicates $p < 0.05$ by Student's *t* test.

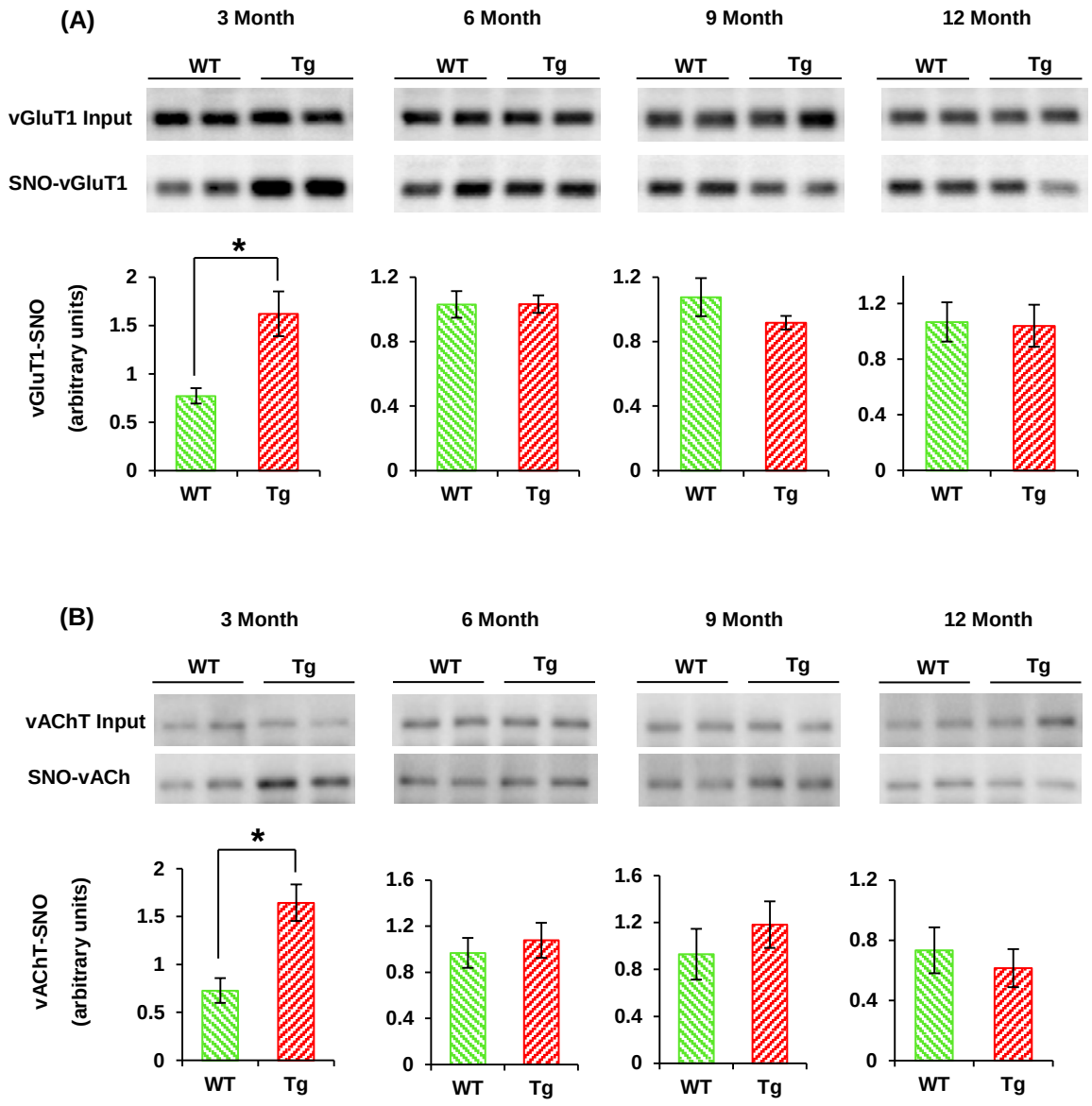

Figure 15. vGluT1 and vAChT S-nitrosylation in hippocampus from Wild Type (WT) mice and APP/PS1 Transgenic (Tg) Mice. vGluT1 S-nitrosylation (vGluT1-SNO) (A) and vAChT S-nitrosylation (vAChT-SNO) (B) were investigated in the hippocampus extracts from all age groups of APP/PS1 and wild type mice. Biotin switch method was employed to switch S-nitrosylated cysteines with biotin. Biotinylated proteins were then precipitated by avidin agarose. Immunoblotting was performed to check the vGluT1 (A) and vAChT (B) with anti-vGluT1 and anti-vAChT antibody. vGluT1 input (A) and vAChT input (B) were used to check the protein equal loading respectively, in which a small amount of samples were separated before precipitation, and then loaded in a separate gel. Data are displayed as mean ± SEM, 3 month: Tg = 10, WT = 9; 6 month: Tg = 6, WT = 10; 9 month: Tg = 9, WT = 9; 12 month: Tg = 5, WT = 9. * indicates $p < 0.05$ by Student's *t* test.

3.4.2 The changes of vGluT1 and vAChT Expression in the frontal cortex and hippocampus from the wild type mice and APP/PS1 transgenic mice.

In Figure 16A, no significant difference of vGluT1 expression was detected between the 3 month APP/PS1 mice and their wild type littermates (0.97 ± 0.06 vs 1.05 ± 0.02, t_{17} = 1.200, p = 0.247); between 9 month APP/PS1 mice and their wild type littermates (1.12 ± 0.07 vs 0.96 ± 0.05, t_{16} = -2.010, p = 0.061); or between 12 month APP/PS1 mice and their wild type littermates (1.28 ± 0.09 vs 1.07 ± 0.07, t_{12} = -1.594, p = 0.137). A significant decrease of vGluT1 expression was only detected in 6 month APP/PS1 mice compared to their wild type littermates (0.82 ± 0.06 vs 1.07 ± 0.04, t_{14} = 2.223, $p < 0.05$). In Figure 16B, no significant difference of vAChT expression was detected between the 3 month APP/PS1 mice and their wild type littermates (0.99 ± 0.02 vs 1.04 ± 0.02, t_{17} = 1.481, p = 0.157); between the 6 month APP/PS1 mice and their wild type littermates (0.96 ± 0.03 vs 1.06 ± 0.04, t_{14} = 1.432, p = 0.172); between the 9 month APP/PS1 mice and their wild type littermates (1.04 ± 0.04 vs 1.01 ± 0.04, t_{16} = -0.622, p = 0.543); or between the 12 month APP/PS1 mice and their wild type littermates (0.99 ± 0.04 vs 1.03 ± 0.04, t_{12} = 0.664, p = 0.519).

Expression changes of vGluT1 and vAChT in the hippocampus extracts of all age groups were investigated respectively. In Figure 17A, no significant difference of vGluT1 expression was detected between 3 month APP/PS1 mice and their wild type littermates (1.01 ± 0.08 vs 1.00 ± 0.07, t_{17} = 0.001, p = 0.999); between 6 month

APP/PS1 mice and their wild type littermates (0.90 ± 0.08 vs 1.00 ± 0.07, $t_{14} = 0.423$, $p = 0.678$); or between 9 month APP/PS1 mice and their wild type littermates (0.97 ± 0.08 vs 1.18 ± 0.09, $t_{16} = 1.729$, $p = 0.104$). However, a significant increase of vGluT1 expression was detected in 12 month APP/PS1 mice group compared to their wild type littermates (0.99 ± 0.02 vs 0.81 ± 0.02, $t_{12} = -2.866$, $p < 0.05$). In Figure 17B, no significant difference of vAChT expression was detected between 3 month APP/PS1 mice and their wild type littermates (0.90 ± 0.05 vs 1.06 ± 0.06, $t_{17} = 1.983$, $p = 0.064$); between 6 month APP/PS1 mice and their wild type littermates (0.94 ± 0.08 vs 1.13 ± 0.07, $t_{14} = 1.645$, $p = 0.121$); between 9 month APP/PS1 mice and their wild type littermates (1.04 ± 0.09 vs 1.07 ± 0.06, $t_{16} = 0.228$, $p = 0.823$); or between 12 month APP/PS1 mice and their wild type littermates (0.85 ± 0.10 vs 0.98 ± 0.07, $t_{12} = 0.634$, $p = 0.539$).

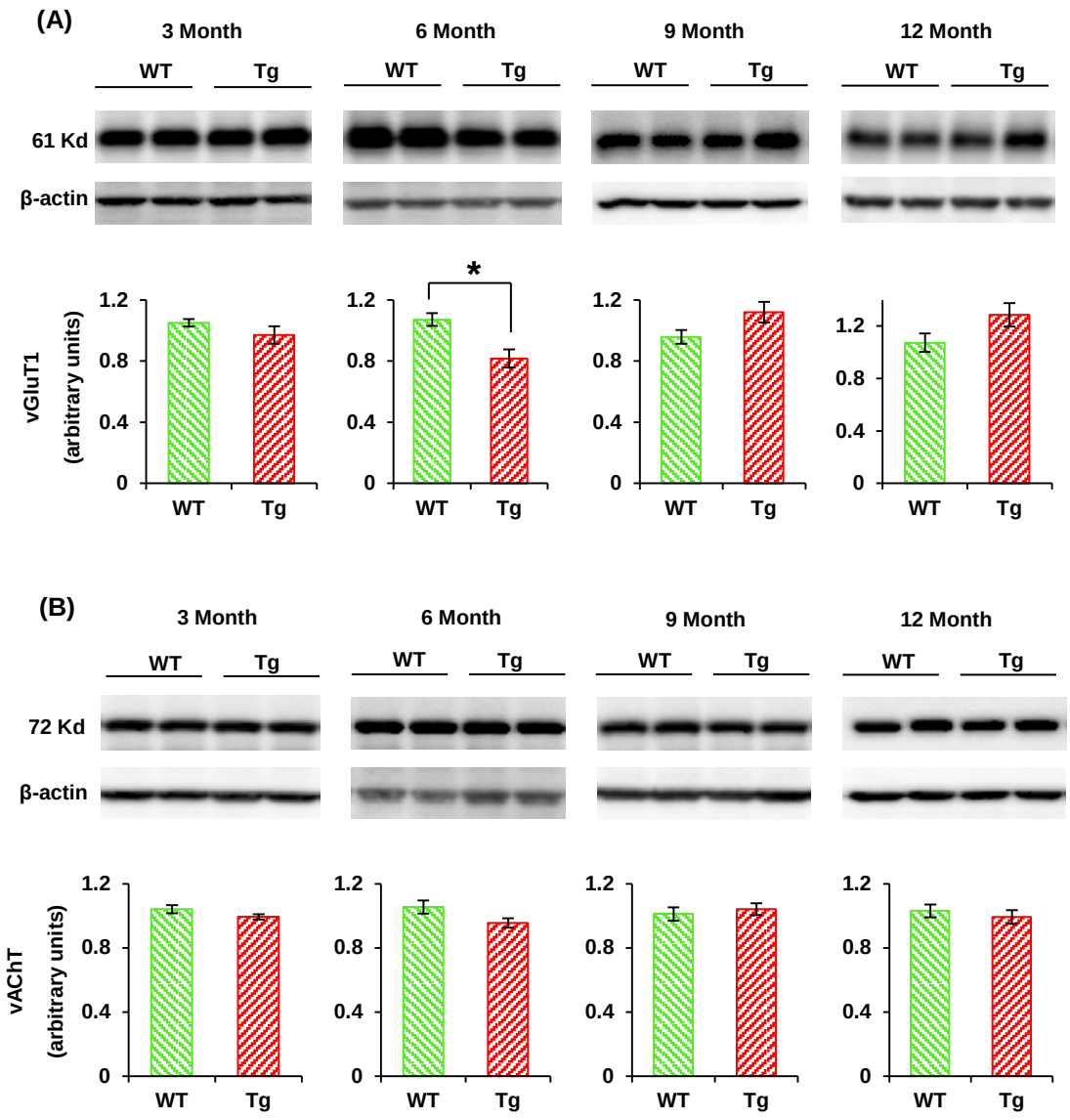

Figure 16. The changes of vGluT1 and vAChT expression in the frontal cortex from the Wild Type (WT) mice and APP/PS1 Transgenic (Tg) mice. vGluT1 expression (A) and vAChT (B) in frontal cortex extracts from all ages were detected by western blot. β-actin was determined to show the equal loading of immunoblotting. Data are displayed as mean ± SEM, 3 month: Tg = 10, WT = 9; 6 month: Tg = 6, WT = 10; 9 month: Tg = 9, WT = 9; 12 month: Tg = 5, WT = 9. * indicates $p < 0.05$ by Student's *t* test.

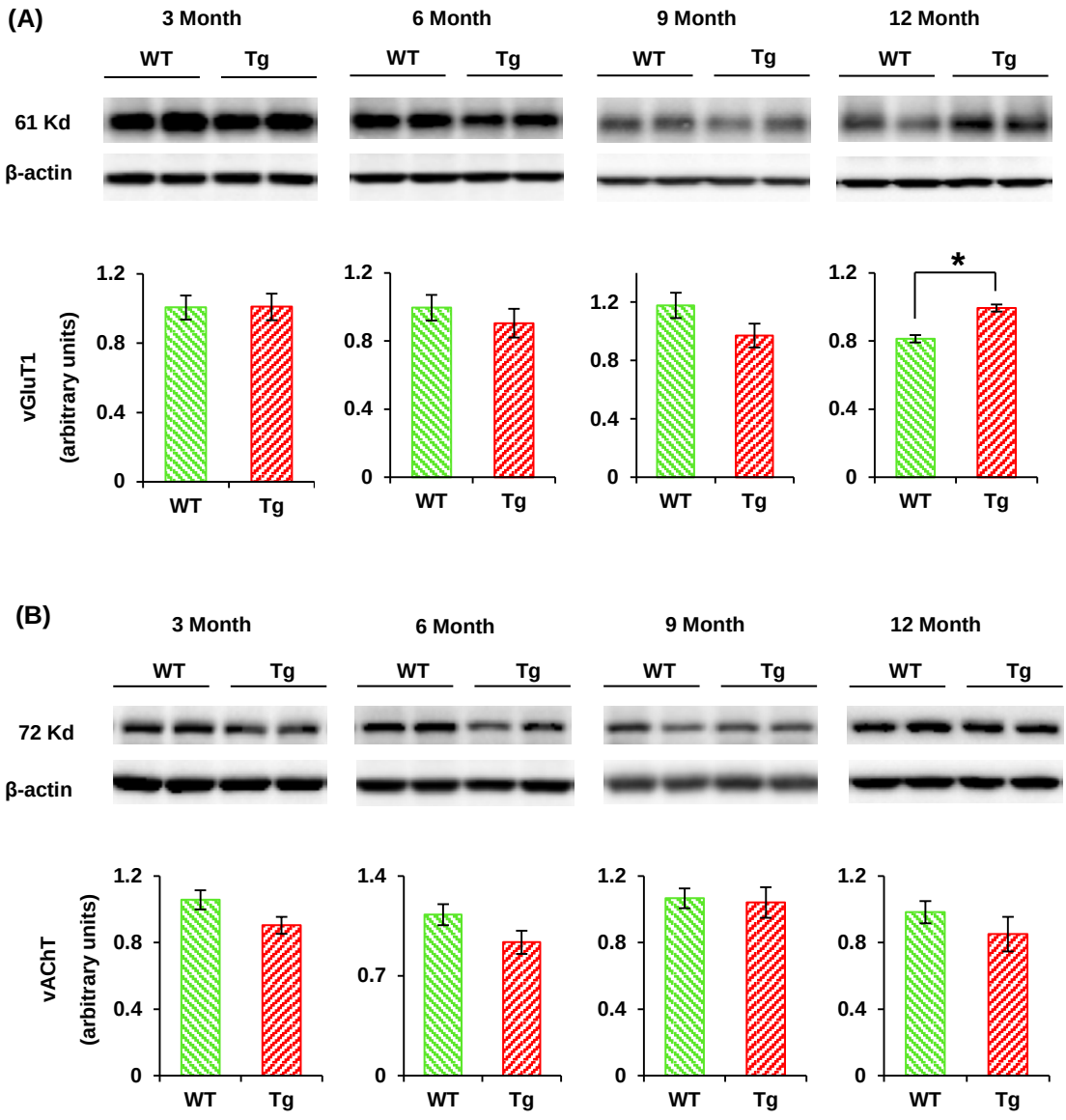

Figure 17. The changes of vGluT1 and vAChT expression in the hippocampus from the Wild Type (WT) mice and APP/PS1 Transgenic (Tg) mice. vGluT1 expression (A) and vAChT (B) in hippocampus extracts from all ages were detected by western blot. β-actin was determined to show the equal loading of immunoblotting. Data are displayed as mean ± SEM, 3 month: Tg = 10, WT = 9; 6 month: Tg = 6, WT = 10; 9 month: Tg = 9, WT = 9; 12 month: Tg = 5, WT = 9). * indicates $p < 0.05$ by Student's *t* test.

CHAPTER 4: DISCUSSION

4.1 Vesicular transporters could be S-nitrosylated

In the present studies, we found that NO donor GSNO at high concentrations (> 10 μM) not only increased S-nitrosylation of vAChT, vMAT2, vGluT1 and vGluT2, but also inhibited vesicular uptake of [^{3}H]acetylcholine, [^{3}H]dopamine and [^{3}H]glutamate. These results suggest that vAChT, vMAT2, vGluT1 and vGluT2 can be S-nitrosylated and that S-nitrosylation of these transporters may further suppress transporter uptake activities.

S-nitrosylation is a posttranscriptional modification. S-nitrosylation of vAChT, vMAT2, vGluT1 and vGluT2 suggests that these transporters can be post-transcriptionally modified. Indeed, protein structure analysis has implicated multiple post-transcriptional modification sites for vAChT, vMAT2, vGluT1 and vGluT2, including sites of oxidation, phosphorylation and glycosylation [156]. Within these modifications, Ser480 of vAChT and the distal C-terminal of vMAT2 can be phosphorylated in monkey kidney transfected COS cells. Phosphorylation of vAChT and vMAT2 were found to regulate their trafficking events, by which blockade of the phosphorylation disrupts the localization of vAChT and vMAT2 to vesicles in PC12 cells [155]. These findings, together with our findings, suggest that vAChT, vMAT2, vGluT1 and vGluT2 may undergo multiple forms of posttranscriptional modifications.

Protein S-nitrosylation plays important roles in cellular signaling mechanism, as it is a reversible and selective process. Many studies have shown that S-nitrosylation can regulate functions of various proteins in neuronal system, and most of these studies were reported on enzymes [33,83,112,115,122]. In general, S-nitroyslation may increase or decrease protein (enzyme) activity, leading to higher or lower efficiency of their function. For instance, S-nitrosylation of Cys83 and Cys157 in Cdk5 can increase the Cdk5 activity, leading to hyperactivity of NMDA receptors and ultimately spine loss [130]; S-nitrosylation of PDI decreases its chaperone activity and isomerase activity, which leads to accumulated protein aggregation and ER stress [125,126]. S-nitrosylation of vAChT, vMAT2, vGluT1 and vGluT2 may also regulate their transport activities and efficiency. vAChT, vGluT1, vMAT2 and vGluT2 contain many cysteine residues with 8 cysteines in vAChT, 10 cysteines in vMAT2, 12 cysteines in vGluT1 and 9 cysteines in vGluT2 [156]. These cysteine residues have potential to be modulated by S-nitrosylation when exposed to an environment with high concentration of NO. For example, structure analysis of vGluTs indicated the loops between transmembrane domains (TMs) 6-7 and 8-9, and regions C-terminal to TM2 and N-terminal to TM3 are exposed to the cytosol [157], which are accessible for posttranscriptional modifications. Within vGluTs, 9/12 in vGluT1 and 5/9 in vGluT2 are within transmembrane domains. This indicates a high chance of cysteine residues to be S-nitrosylated. Until now no direct evidence has been reported that cysteine is responsible for the transport ability of vesicular transporters, however, cysteine was found to regulate binding of certain compound in the transporters,

for instance, in human vMAT2, it is reported that Cys439 in TM 11 was the primary tetrabenazine (TBZ)-protectable target that mediates dihydrotetrabenazine (TBZOH) binding [158]. Another important function of cysteine is that it might influence the functions of vesicular transporters by changing their structures, as it is previously reported that Cys126 in loop 1/2 and Cys333 in loop 7/8 of human vMAT2 forms a disulfide bond [159]. Considering the important roles that disulfide bond plays in protein stabilization and protein function, occupation of cysteines caused by S-nitrosylation may inhibit these bond formations. Therefore, we suggest that S-nitrosylation of cysteine residues in vAChT, vMAT2, vGluT1 and vGluT2 changes the structure of these proteins, thus lowering the transport efficiency.

To determine the functional changes caused by S-nitrosylation of these vesicular transporters, uptake of neurotransmitters were further investigated. Our result demonstrated that GSNO at high concentrations inhibited the vesicular uptake of [^{3}H]acetylcholine, [^{3}H]dopamine and [^{3}H]glutamate, indicating that S-nitrosylation of vAChT, vMAT2, vGluT1 and vGluT2 may further down-regulate transporter uptake activities. This is supported by recent evidence that S-nitrosylated vMAT2 inhibits dopamine uptake. In this study, METH significantly decreased DA content of vesicles from the striatum of rats after drug administration compared to control, while nNOS inhibitor S-methyl-L-thiocitrulline (SMTC) partially attenuated the METH-induced decrease in vesicular DA content [165]. Biotin switch method further revealed a

significant higher S-nitrosylated vMAT2 in the METH-administrated striatal vesicle fractions. This study indicates an inhibitory effect of vMAT2 S-nitrosylation on dopamine uptake. Combine the previous result that vAChT, vMAT2, vGluT1 and vGluT2 can be S-nitrosylated, therefore, we suggest that S-nitrosylation of vesicular transporters inhibits the uptake of neurotransmitters.

S-nitrosylation of various presynaptic proteins may inhibit neurotransmission. Vesicles are the carriers for neurotransmitters, thus the normal functions of vesicular proteins are crucial for health neurotransmission. Recently it is reported that NO has a long-lasting inhibition on presynaptic metabolism and neurotransmitter release by protein S-nitrosylation [159]. Biotin switch method result demonstrated a significant increase of total S-nitrosylated vesicular proteins by high concentrations of NO donors (more than 100 μM) including spermine–nitric oxide complex (NONOate), Z-1-N-methyl-N-[6-(N-methylammoniohexyl)amino]diazen-1-ium-1,2-diolate (MAHMA NONOate), S-nitroso-L-cysteine, and 3-Morpholinylsydnoneimine (SIN-1) in rat forebrain synaptosomes. Further study demonstrated that these NO donors inhibited vesicular component of glutamate release and this inhibitory effect persisted for more than 1 h. This result was in an order of potency that closely matched levels of glutamate release [159]. Other studies also support this viewpoint, for example, NO donors at 100 μM increased the S-nitrosylation of norepinephrine transporters (NET) at Cys351, which further inhibits the reuptake of NE into the pre-synapse in Chinese hamster ovary (CHO)

cells [160]. This study indicates a crucial role of presynaptic proteins including vesicular transporters in neurotransmission, and S-nitroylation of presynaptic proteins may contribute to the deficits of neurotransmission.

4.2 S-nitrosylation of vGluT1 and vAChT in brain of APP/PS1 mice

The APP/PS1 mouse model has long been used for the investigation of behavioral and pathological changes for AD [61-70]. In the current study, using Morris water maze test we found that the latency is significantly increased and the swimming crossings passing platform area were significantly decreased in 9 and 12 month old APP/PS1 double transgenic mice. Using Y maze test we also found that the repetitive entries in each three consecutive crossings are significantly increased in 3 month APP/PS1 transgenic mice. These results are consistent with previous studies [61,63-69], indicating that short term memory is impaired in 3 month APP/PS1 transgenic mice, while spatial memory is impaired in 9 and 12 month APP/PS1 mice.

Our study also demonstrated a significant increased total protein S-nitrosylation in the frontal cortex and hippocampus of the 9 and 12 month APP/PS1 mice. Although increased protein S-nitrosylation has been found in some other AD models such as Tg2526 and Aβ cell models [33,34,110,125,131], this finding was the first time to show that protein S-nitrosylation is significantly increased in brain of APP/PS1 transgenic mice.

Since Aβ has been reported to be consistently increased in 9 and 12 month old APP/PS1 transgenic mice when compared to wild-type controls, our findings suggest that protein S-nitrosylation may be caused by increased Aβ in APP/PS1 transgenic mice. These studies suggest that S-nitrosylation process may contribute to pathology of AD.

S-nitrosylation is induced by NO radicals. Many studies have shown that Aβ can increase NO production. It was reported that exposure to oligomeric $A\beta_{1-42}$ leads to a significant increase in NO production while nNOS inhibitor L-NAME completely eliminated Aβ-triggered NO production in cultured rat cerebrocortical neurons [162]. Swedish double mutation APP (APPsw) transfected cells exhibit substantial high Aβ levels. In PC12 cells and HEK cells transfected with this mutation, NO levels and nNOS activity were increased, while both increased NO level and nNOS activitity were inhibited by inhibiting γ-secretase activity [162]. In addition, Aβ oligomers can activate iNOS in glial cells, generating high levels of NO [87,106,109]. In animal models, when $A\beta_{1-42}$ was injected into temporal cortex of rats, an increased nNOS expression in the same brain was detected [164]. Injection of $A\beta_{25-35}$ into rat temporal cortex not only caused a significant increase of iNOS expression but also reduced spatial memory in these rats. Furthermore, the Aβ-triggered NO production is closely related to hyperactivity of extrasynaptic NMDA receptors rather than synaptic NMDA receptors [33,110,160,163,]. This is explained in the studies that by using NMAD receptor inhibitors, nNOS activity can be significantly lowered [87,106,109]. In AD, Aβ toxicity triggers hyperactivity of NMDA receptors,

leading to an increased Ca^{2+} influx. Increased intracellular calcium then activates nNOS, leading to elevated NO production [106-108]. On the other hand, Aβ oligomers can activate iNOS in glial cells, generating high levels of NO [87,106,109]. In our animal model, we suggest that increased protein S-nitrosylation is caused by soluble Aβ toxicity, might through activation of NOSs. We also found that APP/PS1transgenic mice at these ages showed reduced spatial memory and increased protein S-nitrosylation in brain. These studies together suggest that Aβ may activate NOSs, subsequently resulting in increased production of NO radicals and that NO-induced protein S-nitrosylation may play a role in memory loss in AD.

Significantly increased total protein S-nitrosylation may trigger various neurodegeneration pathways, contributing to the cognitive changes in APP/PS1 mice. As reported in a high through proteomic studies, more than 100 proteins have been identified to be S-nitrosylated in transgenic mouse model overexpressing mutated human APP and in post mortem brain tissue of AD patients [34]. The vast majority of S-nitrosylated proteins are related to synaptic loss, apoptosis, energy metabolism and redox regulation [34,131]. Synapses as the main sites for signal connection, are essential for healthy neurotransmission. Recently 138 synaptic proteins were reported to be S-nitrosylated in transgenic mice overexpressing mutated human APP (hAPP), such as membrane-associated guanylate kinases (MAGUK), CamkII and synaptotagmins [131], indicating that synaptic proteins are easily accessible to NO modification in AD. Though

the S-nitrosylation role of most of these proteins have not been explained, some proteins already gave us clues on the detrimental effect on neurotransmission. For instance, Cdk5 is a cyclin-dependent kinase has been implicated in multiple processes including axon guidance, neuronal migration, neuronal survival and the regulation of synaptic spine density [62,63,64]. Hyperactivity of Cdk5 triggered by a number of stimulus (including oxidative stress, Aβ exposure, calcium overload) contributes to neuronal death in AD. Recently it is reported that S-nitrosylation of Cdk5 is significantly increased in cells treated with $A\beta_{1-42}$ oligomers and in AD post mortem brains. In vitro study demonstrated a significant increase of spine loss in the same cell model when exposed to NO donors or $A\beta_{1-42}$ oligomers, while both the spine loss and Cdk5 S-nitrosylation can be obligated by NNA treatment (NOS inhibitor) [33]. Other proteins such as Drp1, IDE and PDI could also increase synapse loss by S-nitrosylaion, but through different signaling pathways [110,113,114,122,125,126].

Our study also showed that although protein levels of vGluT1 and vAChT were not different in brain between APP/PS1 transgenic mice and age-matched wild-type controls, S-nitrosylation of vAChT and vGluT1 was increased in frontal cortex of 6, 9 and 12 month old APP/PS1 mice. S-nitrosylation of vAChT and vGluT1 was also increased in hippocampus of 3 month APP/PS1 mice. Our study suggests that S-nitrosylation of vAChT and vGluT1 may contribute a part to impairment of cholinergic and glutamatergic systems identified in AD. Because we also found that NO radicals can inhibit vesicular

acetylcholine and glutamate uptake, our study suggests that *S*-nitrosylation of vAChT and vGluT1 may further inhibit vAChT and vGluT1 activities in brain of this AD animal model.

Protein S-nitrosylation of vAChT might interfere neurotransmission process of cholinergic system. Many studies have indicated that in AD, cholinergic system is impaired, and that cholinergic deficits mainly result from decreased acetylcholine and death of cholinergic neurons. It has been found that low concentrations of exogenous $A\beta_{1\text{-}40}$ or $A\beta_{25\text{-}35}$ acutely inhibited endogenous acetylcholine release from the rat hippocampus from neuromuscular junctions [166,167]. Microdialysis study showed that high K^+-evoked acetylcholine release was decreased while the spontaneous release of acetylcholine was not significantly decreased by treatment of Aβ oligomers [168]. No direct evidence has been reported that S-nitrosylation of vesicular proteins inhibits the uptake of acetylcholine. However, cholinergic deficits caused by Aβ toxicity have been reported as one of the hallmarks of AD. Protein S-nitrosylation is also an important neuropathological process to induce synaptic loss and neuronal cell death as explained previously. Moreover, in our previous result, S-nitrosylation could inhibit the uptake of acetylcholine. Therefore, we suggest that cholinergic deficits might be, at least partially attributed to the increased S-nitrosylation of various synaptic proteins. In the current study, we found both increased S-nitrosylation of vAChT and decreased learning and memory

in 9 and 12 month old APP/PS1 mice, suggesting a potential inhibitory role of S-nitrosylation of vAChT on cognitive changes.

Increased S-nitrosylation of vGluT1 in APP/PS1 mice may also impair glutamatergic neurotransmission. Because we also found that NO radical inhibited vesicular glutamate uptake, our results indicate that S-nitrosylation of vGluT1 may inhibit vGluT1 activity and cause accumulation of glutamate in cytosol. Studies have shown that accumulated glutamate can be reversely transported out of pre-synapse mediated by EAAT3 [176,177]. EAAT3 is located in axon terminals. Under physiological conditions, extracellular glutamate can be uptaken by presynapse through EAAT3 and then re-uptaken by synaptic vesicles. However, under pathological conditions such as ischemic condition, EAAT3 can reversely transport glutamate and cause exitotoxicity [177]. These studies together suggest that increased Aβ in APP/PS1 mice may induce S-nitrosylation of vGluT1, resulting in inhibition of vGluT1. Inhibited vGluT1 can decrease vesicular uptake of glutamate and increase cytosolic glutamate levels. Accumulated cytosolic glutamate may be further transported reversely out of pre-synapse, resulting in the elevated extracellular glutamate levels. Indeed, many studies have shown that Aβ can induce extracellular glutamate levels. For example, intracerebral injection with low concentrations of soluble Aβ in rats can increase the glutamate release from prefrontal cortex of rat cortex or hippocampal slices [169,170]. In animal models, elevated glutamate

induced by Aβ toxicity is associated with increased cognitive impairments [171-175]. Elevated extracellular glutamate has also been found in 7 month APP/PS1 transgenic mice.

In AD, Aβ toxicity is able to trigger multiple pathological conditions, such as oxidative/nitrosative stress, neuronal excitotoxicity and so forth, which might trigger reversed EAAT3 transport. The S-nitrosylation of vGluT1 in our study has been shown to inhibit the uptake of glutamate, contributing to an increased intracellular glutamate that might be released into the synaptic clefts. Here we suggest S-nitrosylation of vGluT1 might contribute to glutamate release through reversed transport through EAAT3, however, further study is needed to verify this suggestion.

4.3 Limitations of the study

In the study, there are several limitations. First, S-nitrosylation is a reversible and specific posttranslational modification, which is also a redox-sensitive and labile protein modification. Therefore, endogenous S-nitrosylation detection is technically more challenging than some other modifications such as phosphorylation and carbonylation. Protein input used in the study as equal loading might not best show the real loading of the samples. The S-nitrosylated thiol group is liable and light sensitive, which makes it difficult to detect. False positive signal may come from endogenous biotinylation, and incomplete blocking. So we tried to modify the method by prolonging the blocking time

and increased the concentration of reducing agent. We tried to repeat the experiment for at least 4 times for the *in vitro* study and repeat 2 times for the animal study.

The second limitation in this study is the uptake variance of [^{3}H] acetylcholine, which might be caused by the degradation effect from cholinesterase on the postsynaptic membranes. In the study, crude vesicles were isolated and used for the experiment, in which a certain amount of membranes could be detected in Figure 5 (vesicle isolation), indicating a potential effect of cholinesterase on acetylcholine degradation. In the experiment, paroxon, a cholinesterase inhibitor, was used to inhibit the cholinesterase activity.

Finally, the animal number is limited in 6 month and 12 month groups. The animals died in these two groups due to fight, in which only 6 APP/PS1 mice remained in 6 month group and 5 remained in 12 month group before behavioral study. And the variation of the mouse performance led to a problem when analyzing the data in these two groups.

CHAPTER 5: CONCLUSIONS AND FUTURE DIRECTIONS

5.1 Overall conclusions

In the present studies, we found that:

1. NO radicals can induce S-nitrosylation of vAChT, vMAT2 and vGluTs, and also inhibit vesicular uptake of acetylcholine, dopamine and glutamate.

2. Learning and memory are decreased and total brain protein S-nitrosylation is increased in 9 month and 12 month old APP/PS1 transgenic mice.

3. S-nitrosylation of vAChT and vGluT1 is increased in the hippocampus of 3 month old APP/PS1 transgenic mice, and S-nitrosylation of vAChT and vGluT1 is increased in the frontal cortex of 6, 9 and 12 month old APP/PS1 transgenic mice.

These findings suggest that S-nitrosylation of vAChT and vGluT1 inhibits the uptake of acetylcholine and glutamate, and might be implicated for the cholinergic and glutamatergic dysfuntion in AD.

5.2 Significance of this research

Cysteine residues in proteins are sensitive to ROS/RNS attack and undergo reversible

and irreversible oxidative modifications. Oxidative cysteine S-nitrosylation modulates protein function, enzyme activity and neurodegeneration. Our current findings help understanding the role that reversible cysteine oxidative modification plays in AD pathology. These findings also indicate that S-nitrosylation process may be a potential target for the treatment of AD and other dementias.

5.3 Future directions

To determine whether Aβ is a factor for the increased protein S-nitrosylation in APP/PS1 transgenic mice, we will use Aβ oligomers to treat mouse hippocampal HT22 cells. The effect of Aβ oligomers on S-nitrosylation of vAChT and vGluT1 will be investigated. Meanwhile the effect of Aβ oligomers on vesicular acetylcholine and glutamate will also be detected. We will also investigate whether Trx, one of the main antioxidants in the human body, can reverse the protein S-nitrosylation induced by GSNO or Aβ oligomers in HT22 cells.

We will also investigate the levels of Trx/TrxR in the brain of APP/PS1 mice and their wild type littermates, to find the role that Trx/TrxR play in nitrosative process. It will also be an interesting to deliver Trx/TrxR in the transgenic mouse brains to see the behavioral changes. This will give us a new understanding on the pharmacological treatment for Alzheimer's disease.

To date, the biotin switch method is a very popular method used to detect S-nitrosylated proteins. However, some technical limitations could not be solved as described above. Recently, some new methods have been developed which are more precise and more stable, such as Mass Spectrometry and high throughput proteomic measurement. We will apply the new methods to address the limitations of conventional biotin switch method to detect S-nitrosylated proteins in synapse extracts from APP/PS1 mice.

BIBLIOGRAPHY

[1] Kenche, V. B., & Barnham, K. J. (2011). Alzheimer's disease & metals: therapeutic opportunities. *Br J Pharmacol, 163*(2), 211-9.

[2] Hebert, L. E., Scherr, P. A., Bienias, J. L., Bennett, D. A., & Evans, D. A. (2004). State-specific projections through 2025 of Alzheimer diseaseprevalence. *Neurology, 62*(9), 1645.

[3] LaFerla, F. M., Green, K. N., & Oddo, S. (2007). Intracellular amyloid-β in Alzheimer's disease. *Nat Rev Neurosci, 8*(7), 499–509.

[4] Selkoe, D. J. (2002). Alzheimer's disease is a synaptic failure. *Science, 298*(5594), 789–91.

[5] Terry, R. D., Masliah, E., Salmon, D. P., Butters, N., DeTeresa, R., Hill, R., et al. (1991). Physical basis of cognitive alterations in Alzheimer's disease: synapse loss is the major correlate of cognitive impairment. *Ann Neurol, 30*(4):572–80.

[6] Kumar, S., & Walter, J. (2011). Phosphorylation of amyloid beta (Aβ) peptides-a trigger for formation of toxic aggregates in Alzheimer's disease. *Aging, 3*(8), 803-12.

[7] Gozes, I. (2010). Tau pathology and future therapeutics. *Curr Alzheimer Res, 7*(8), 685-6.

[8] Chun, W., & Johnson, G. V. (2007). The role of tau phosphorylation and cleavage in neuronal cell death. *Front Biosci, 12*, 733-56.

[9] Goate, A., Chartier, H. M. C., Mullan, M., Brown, J., Crawford, F., Fidani, L., et al. (1991). Segregation of a missense mutation in the amyloid precursor protein gene with familial Alzheimer's disease. *Nature, 349*(6311), 704-6.

[10] Rohan, de S., H. A., Jen, A., Wickenden, C., Jen, L. S., Wilkinson, S. L., & Patel, A. J. (1997). Cell-specific expression of beta-amyloid precursor protein isoform mRNAs and proteins in neurons and astrocytes. *Brain Res Mol Brain Res*, *47*(1-2), 147-56.

[11] Kang, J., & Muller, H. B. (1990). Differential splicing of Alzheimer's disease amyloid A4 precursor RNA in rat tissues: PreA4(695) mRNA is predominantly produced in rat and human brain. *Biochem Biophys Res Commun, 166*(3), 1192-200.

[12] Zhang, Y. W., Thompson, R., Zhang, H., & Xu, H. (2011). APP processing in Alzheimer's disease. *Mol Brain, 4*, 3.

[13] Liu, Y., Zhang, Y. W., Wang, X., Zhang, H., You, X., Liao, F. F., et al. (2009). Intracellular trafficking of presenilin 1 is regulated by beta-amyloid precursor

protein and phospholipase D1. *J Biol Chem*, *284*(18), 12145-52.

[14] Sisodia, S. S. (1992). Beta-amyloid precursor protein cleavage by a membrane-bound protease. *Proc Natl Acad Sci USA*, *89*(13), 6075-9.

[15] De Strooper, B., Iwatsubo, T., & Wolfe, M. S. (2012). Presenilins and gamma-secretase: structure, function, and role in Alzheimer Disease. *Cold Spring Harb Perspect Med*, *2*(1), a006304.

[16] Haass, C., Kaether, C., Thinakaran, G., & Sisodia, S. (2012). Trafficking and proteolytic processing of APP. *Cold Spring Harb Perspect Med*, *2*(5), a006270.

[17] Zeiger, W., Vetrivel, K. S., Buggia, P. V., Nguyen, P. D., Wagner, S. L., Villereal, M. L., et al. (2013). Ca^{2+} influx through store-operated Ca^{2+} channels reduces Alzheimer disease β-amyloid peptide secretion. *J Biol Chem*, *288*(37), 26955-66.

[18] Furukawa, K., Sopher, B. L., Rydel, R. E., Begley, J. G., Pham, D. G., Martin, G. M., et al. (1996). Increased activity-regulating and neuroprotective efficacy of alpha-secretase-derived secreted amyloid precursor protein conferred by a C-terminal heparin-binding domain. *J Neurochem*, *67*(5), 1882-96.

[19] Mattson, M. P. (1997). Cellular actions of beta-amyloid precursor protein and its soluble and fibrillogenic derivatives. *Physiol Rev*, *77*(4), 1081-132.

[20] Tamayev, R., Zhou, D., & D'Adamio, L. (2009). The interactome of the amyloid beta precursor protein family members is shaped by phosphorylation of their intracellular domains. *Mol Neurodegener*, *4*, 28.

[21] Baek, S. H., Ohgi, K. A., Rose, D. W., Koo, E. H., Glass, C. K., & Rosenfeld, M. G. (2002). Exchange of N-CoR corepressor and Tip60 coactivator complexes links gene expression by NF-kappaB and beta-amyloid precursor protein. *Cell*, *110*(1), 55-67.

[22] Kim, H. S., Kim, E. M., Lee, J. P., Park, C. H., Kim, S., Seo, J. H., et al. (2003). C-terminal fragments of amyloid precursor protein exert neurotoxicity by inducing glycogen synthase kinase-3beta expression. *FASEB J*, *17*(13), 1951-3.

[23] Pardossi, P. R., Petit, A., Kawarai, T., Sunyach, C., Alves, C. C., Vincent, B., et al. (2005). Presenilin-dependent transcriptional control of the Abeta-degrading enzyme neprilysin by intracellular domains of betaAPP and APLP. *Neuron*, *46*(4), 541-54.

[24] von Rotz, R. C., Kohli, B. M., Bosset, J., Meier, M., Suzuki, T., Nitsch, R. M., et al. (2004). The APP intracellular domain forms nuclear multiprotein complexes and regulates the transcription of its own precursor. *J Cell Sci*, *117*(Pt 19), 4435-48.

[25] Zhang, Y. W., Wang, R., Liu, Q., Zhang, H., Liao, F. F., & Xu, H. (2007). Presenilin/gamma secretase-dependent processing of beta-amyloid precursor protein regulates EGF receptor expression. *Proc Natl Acad Sci USA, 104*(25), 10613-8.

[26] Liu, Q., Zerbinatti, C. V., Zhang, J., Hoe, H. S., Wang, B., Cole, S. L., et al. (2007). Amyloid precursor protein regulates brain apolipoprotein E and cholesterol metabolism through lipoprotein receptor LRP1. *Neuron, 56*(1), 66-78.

[27] Vassar, R., Kovacs, D. M., Yan, R., & Wong, P. C. (2009). The beta-secretase enzyme BACE in health and Alzheimer's disease: regulation, cell biology, function, and therapeutic potential. *J Neurosci, 29*(41), 12787-94.

[28] Nikolaev, A., McLaughlin, T., O'Leary, D. D., & Tessier, L. M. (2009). APP binds DR6 to trigger axon pruning and neuron death via distinct caspases. *Nature, 457*(7232), 981-9.

[29] Walsh, D. M., & Selkoe, D. J. (2004). Oligomers on the brain: the emerging role of soluble protein aggregates in neurodegeneration. *Protein Pept Lett, 11*(3), 213-28.

[30] Volles, M. J., & Lansbury, P. T. Jr. (2002). Vesicle permeabilization by protofibrillar alpha-synuclein is sensitive to Parkinson's disease-linked mutations and occurs by a pore-like mechanism. *Biochemistry, 41*(14), 4595-602.

[31] Glabe, C. C. (2005). Amyloid accumulation and pathogensis of Alzheimer's disease: significance of monomeric, oligomeric and fibrillar Abeta. *Subcell Biochem, 38*, 167-77.

[32] Crews, L., & Masliah, E. (2010). Molecular mechanisms of neurodegeneration in Alzheimer's disease. *Hum Mol Genet, 19*(R1), R12-20.

[33] Qu, J., Nakamura, T., Cao, G., Holland, E. A., McKercher, S. R., & Lipton, S. A. (2011). S-Nitrosylation activates Cdk5 and contributes to synaptic spine loss induced by beta-amyloid peptide. *Proc Natl Acad Sci USA, 108*(34), 14330–5.

[34] Zahid, S., Khan, R., Oellerich, M., Ahmed, N., & Asif, A. R. (2013). Differential S-nitrosylation of proteins in Alzheimer's disease. *Neuroscience, 256*, 126–36.

[35] Westermann, B. (2009). Nitric oxide links mitochondrial fission to Alzheimer's disease. *Sci Signal, 2*(69), pe29.

[36] Knott, A. B., & Perkins, G., Schwarzenbacher, R., Bossy, W. E. (2008). Mitochondrial fragmentation in neurodegeneration. *Nat Rev Neurosci, 9*(7), 505–18.

[37] Tiraboschi, P., Sabbagh, M. N., Hansen, L. A., Salmon, D. P., Merdes, A., Gamst, A., et al. (2004). Alzheimer disease without neocortical neurofibrillary tangles: a

second look. *Neurology*, *62*(7), 1141-7.

[38] Takashima, A., Honda, T., Yasutake, K., Michel, G., Murayama, O., Murayama, M., et al. (1998). Activation of tau protein kinase I/glycogen kinase-3beta by amyloid beta peptide (25-35) enhances phosphorylation of tau in hippocampal neurons. *Neurosci Res*, *31*(4), 317-23.

[39] Bartus, R. T., Dean, R. L., Beer, B., & Lippa, A. S., (1982). The cholinergic hypothesis of geriatric memory dysfunction. *Science*, *217*(4558), 408-14.

[40] Klingner, M., Apelt, J., Kumar, A., Sorger, D., Sabri, O., Steinbach, J., et al. (2003). Alterations in cholinergic and non-cholinergic neurotransmitter receptor densities in transgenic Tg2576 mouse brain with beta-amyloid plaque pathology. *Int J Dev Neurosci*, *21*(7), 357-69.

[41] Parent, M. J., Bedard, M. A., Aliaga, A., Minuzzi, L., Mechawar, N., et al. (2013). Cholinergic Depletion in Alzheimer's Disease Shown by [(18)F]FEOBV Autoradiography. *Int J Mol Imaging*, 2013, 205045.

[42] Lodish, H., Berk, A., Zipursky, S. L., et al. (2000). Molecular Cell Biology 4th edition. W. H. Freeman.

[43] Sultana, R., & Butterfield, D. A. (2008). Alterations of some membrane transport proteins in Alzheimer's disease: role of amyloid beta-peptide. *Mol Biosyst*, *4*(1), 36-41.

[44] Auld, D. S., Kornecook, T. J., Bastianetto, S., & Quirion, R. (2002). Alzheimer's disease and the basal forebrain cholinergic system: Relations to [beta]-amyloid peptides, cognition, and treatment strategies. *Prog Neurobiol*, *68*(3), 209–45.

[45] Antonio, C. (2011). The history of the cholinergic hypothesis. *Behav Brain Res*, *221*(2), 334–40.

[46] Mesulam, M. (2004). The cholinergic lesion of Alzheimer's disease: Pivotal factor or side show? *Learn Mem*, *11*(1), 43–9.

[47] Sarter, M., Hasselmo, M. E., Bruno, J. P., & Givens, B. (2005). Unraveling the attentional functions of cortical cholinergic inputs: Interactions between signal-driven and cognitive modulation of signal detection. *Brain Res Brain Rev*, *48*(1), 98–111.

[48] Bierer, L. M., Haroutunian, V., Gabriel, S., Knott, P. J., Carlin, L. S., Purohit, D. P., et al. (1995). Neurochemical correlates of dementia severity in Alzheimer's disease: Relative importance of the cholinergic deficits. *J of Neurochem*, *64*(2), 749–60.

[49] Reinikainen, K. J., Soininen, H., & Riekkinen, P. J. (1990). Neurotransmitter changes in Alzheimer's disease: Implications to diagnostics and therapy. *J*

Neurosci Res, *27*(4), 576–86

[50] Dodd, P. R., Scott, H. L., & Westphalen, R. I. (1994). Excitotoxic mechanisms in the pathogenesis of dementia. *Neurochem Int*, *25*(3), 203–19.

[51] Watkins, J. C., & Evans, R. H. (1981). Excitatory amino acid transmitters. *Annu Rev Pharmacol Toxicol*, *21*, 165–204.

[52] Chen, K. H., Reese, E. A., Kim, W., Rapoport, S. I., & Rao, J. S. (2011). Disturbed Neurotransmitter Transporter Expression in Alzheimer's Disease Brain. *J Alzheimers Dis*, *26*(4), 755–66.

[53] Francis, P. T. (2005). The interplay of neurotransmitters in Alzheimer's disease. *CNS Spectr*, *10*(11 Suppl), 6-9.

[54] Butterfield, D. A., & Pocernich, C. B. (2003). The glutamatergic system and Alzheimer's disease: therapeutic implications. *CNS Drugs*, *17*(9), 641–52.

[55] Wang, Y., & Qin, Z. H. (2010). Molecular and cellular mechanisms of excitotoxic neuronal death. *Apoptosis*, *15*(11), 1382–402.

[56] Kim, K., Lee, S. G., Kegelman, T. P., Su, Z. Z., Das, S. K., Dash, R., et al. (2011). Role of excitatory amino acid transporter-2 (EAAT2) and glutamate in neurodegeneration: opportunities for developing novel therapeutics. *J Cell Physiol*, *226*(10), 2484-93.

[57] Yokoyama, K., Gaulin, N. B., Cho, H., & Briglio, N. M. (2010) Temperature dependence of conjugation of amyloid beta protein on the surfaces of gold colloidal nanoparticles. *J Phys Chem A*, *114*(3), 1521-8.

[58] Takamori, S., Rhee, J. S., Rosenmund, C., and Jahn, R. (2000) Identification of a vesicular glutamate transporter that defines a glutamatergic phenotype in neurons. *Nature*, *407*(6801), 189 –94.

[59] Weihe, E., & Eiden, L. E. (2000) Vesicular amine transporter expression in amine-handling cells of the nervous, endocrine and inflammatory systems. *FASEB J*, *14* (15), 2435–49.

[60] Holcomb, L., Gordon, M. N., McGowan, E., Yu, X., Benkovic, S., Jantzen, P., et al. (1998). Accelerated Alzheimer-type phenotype in transgenic mice carrying both mutant amyloid precursor protein and presenilin 1 transgenes. *Nat Med*, *4*(1), 97-100.

[61] He, J., Xu, H., Yang, X., & Li, X. M. (2006). The effects of chronic administration of quetiapine on the phencyclidine-induced reference memory impairment and release of Bcl-XL/Bax ratio in the posterior cingulate cortex in rats. *Behav Brain Res*, *168*(2), 236-42.

[62] Dineley, K. T., Xia, X., Bui, D., Sweatt, J. D., & Zheng, H. (2002). Accelerated

plaque accumulation, associative learning deficits, and up-regulation of alpha 7 nicotinic receptor protein in transgenic mice co-expressing mutant human presenilin 1 and amyloid precursor proteins. *J Biol Chem*, *277*(25), 22768-80.

[63] Cao, D., Lu, H., Lewis, T. L., & Li, L. (2007) Intake of sucrose-sweetened water induces insulin resistance and exacerbates memory deficits and amyloidosis in a transgenic mouse model of Alzheimer disease. *J Biol Chem*, *282*(50), 36275-82.

[64] Cramer, P. E., Cirrito, J. R., Wesson, D. W., Lee, C. Y., Karlo, J. C., Zinn, A. E., et al. (2012). ApoE-directed therapeutics rapidly clear beta-amyloid and reverse deficits in AD mouse models. *Science*, *335*(6075), 1503-6.

[65] Ding, Y., Qiao, A., Wang, Z., Goodwin, J. S., Lee, E. S., Block, M. L., et al. (2008). Retinoic acid attenuates beta-amyloid deposition and rescues memory deficits in an Alzheimer's disease transgenic mouse model. *J Neurosci*, *28*(45), 11622-34.

[66] Ma, T., Du, X., Pick, J. E., Sui, G., Brownlee, M., & Klann, E. (2012). Glucagon-like peptide-1 cleavage product GLP-1(9-36) amide rescues synaptic plasticity and memory deficits in Alzheimer's disease model mice. *J Neurosci*, *32*(40), 13701-8.

[67] Lalonde, R., Kim, H. D., Maxwell, J. A., & Fukuchi, K. (2005). Exploratory activity and spatial learning in 12-month-old APP(695)SWE/co+PS1/DeltaE9 mice with amyloid plaques. *Neurosci Lett*, *390*(2), 87-92.

[68] Zhang, W., Hao, J., Liu, R., Zhang, Z., Lei, G., Su, C., et al. (2011). Soluble Aβ levels correlate with cognitive deficits in the 12-month-old APPswe/PS1dE9 mouse model of Alzheimer's disease. *Behav Brain Res*, *222*(2), 342-350.

[69] Holcomb, L. A., Gordon, M. N., Jantzen, P., Hsiao, K., Duff, K., & Morgan, D. (1999). Behavioral changes in transgenic mice expressing both amyloid precursor protein and presenilin-1 mutations: lack of association with amyloid deposits. *Behav Genet*, *29*(3), 177–85.

[70] Minkeviciene, R., Banerjee, P., & Tanila, H. (2004). Memantine improves spatial learning in a transgenic mouse model of Alzheimer's disease. *J Pharmacol Exp Ther*, *311*(2), 677-82.

[71] McIntire, S. L., Reimer, R. J., Schuske, K., Edwards, R. H., & Jorgensen, E. M. (1997). Identification and characterization of the vesicular GABA transporter. *Nature*, *389*(6653), 870–6.

[72] Wirz, J. A. (1988). Platelet research in psychiatry. *Experientia*, *44*(2), 145–52.

[73] Sagne', C. E., Mestikaway, S., Isambert, M. F., Hamon, M., Nenry, J. P., Giros, B., et al. (1997). Cloning of a functional vesicular GABA and glycine transporter

by screening of genome databases. *FEBS Lett*, *417*(2), 177–83.

[74] Sattler, R., Xiong, Z., Lu, W. Y., Hafner, M., MacDonald, J. F., & Tymianski, M. (1999). Specific coupling of NMDA receptor activation to nitric oxide neurotoxicity by PSD-95 protein. *Science*, *284*(5421), 1845–8.

[75] Beckman, K. B., & Ames, B. N. (1998). The free radical theory of aging matures. *Physiol Rev*, *78*(2), 547– 81.

[76] Esterbauer, H., Schaur, R. J., & Zollner, H. (1991). Chemistry and biochemistry of 4-hydroxynonenal, malonaldehyde and related aldehydes. *Free Radic BiolMed*, *11*(1), 81-128.

[77] Schaur, R. J. (2003). Basic aspects of the biochemical reactivity of 4-hydroxynonenal. *Mol Aspects Med*, *24*(4-5), 149–59.

[78] Sayre, L. M., Perry, G., & Smith, M. A. (2008). Oxidative stress and neurotoxicity. *Chem Res in Toxicol*, *21*(1), 172–88.

[79] Keller, J. N. (2006). Interplay between oxidative damage, protein synthesis, and protein degradation in Alzheimer's disease. *J Biomed Biotechnol*, *2006*(3), 12129.

[80] Popp, R., Fleming, I., & Busse, R. (1998). Pulsatile stretch in coronary arteries elicits release of endothelium-derived hyperpolarizing factor: a modulator of arterial compliance. *Circ Res*, *82*(6), 696–703.

[81] Ignarro, L.J., Cirino, G., Casini, A., & Napoli, C. (1999). Nitric oxide as a signaling molecule in the vascular system: an overview. *J Cardiovasc Pharmacol*, *34*, 879–86.

[82] Bredt, D. S., & Snyder, S. H. (1990). Isolation of nitric oxide synthetase, a calmodulin- requiring enzyme. *Proc Natl Acad Sci USA*, *87*(2), 682–5.

[83] Knowles, R.G., & Moncada, S. (1994). Nitric oxide synthases in mammals. *Biochem J*, *298*(Pt 2), 249–58.

[84] Stuehr, D. J., (1999). Mammalian nitric oxide synthases. *Biochim Biophys Acta*, *1411*(2-3), 217–30.

[87] Kwak, Y. D., Wang, R., Li, J. J., Zhang, Y. W., Xu, H., & Liao, F. F. (2011). Differential regulation of BACE1 expression by oxidative and nitrosative signals. *Mol Neurodegener*, *6*, 17.

[86] Tanaka, Y., Tang, G., Takizawa, K., Otsuka, K., Eghbali, M., Song, M., et al. (2005). Kv Channels Contribute to Nitric Oxide- and Atrial Natriuretic Peptide-Induced Relaxation of a Rat Conduit Artery. *J Pharmacol Exp Ther*, *317*(1), 341–54.

[87] Fukui, H., & Moraes, C. T. (2008). The mitochondrial impairment, oxidative stress and neurodegeneration connection: reality or just an attractive hypothesis?

Trends Neurosci, *31*(5), 251–6.

[88] Hopper, R. A., & Garthwaite, J. (2006). Tonic and phasic nitric oxide signals in hippocampal long-term potentiation. *J Neurosci*, *26*(45), 11513- 21.

[89] Taqatqeh, F., Mergia, E., Neitz, A., Eysel, U. T., Koesling, D., & Mittmann, T. (2009). More than a retrograde messenger: nitric oxide needs two cGMP pathways to induce hippocampal long-term potentiation. *J Neurosci*, *29*(29), 9344–50.

[90] Green, S. J. (1995). Nitric oxide in mucosal immunity. *Nat Med*, *1*(6), 515-7.

[91] Drew, B., & Leeuwenburgh, C. (2002). Aging and the role of reactive nitrogen species. *Ann N Y Acad Sci*, *959*, 66-81.

[92] Wink, D. A., Miranda, K. M., & Espey, M. G. (2000). Effects of oxidative and nitrosative stress in cytotoxicity. *Semin Perinatol*, *24*(1), 20-23.

[93] Lei, S. Z., Pan, Z. H., Aggarwal, S. K., Chen, H. S., Hartman, J., Sucher, N. J., et al. (1992). Effect of nitric oxide production on the redox modulatory site of the NMDA receptor-channel complex. *Neuron*, *8*(6), 1087-99.

[94] Nakamura, T., Tu, S., Akhtar, M. W., Sunic, C. R., Okamoto, S., & Lipton, S. A. (2013). Aberrant protein s-nitrosylation in neurodegenerative diseases. *Neuron*, *78*(4), 596-614.

[95] He, X., & Ma, Q. (2009). NRF2 cysteine residues are critical for oxidant/electrophile-sensing, Kelch-like ECH-associated protein-1-dependent ubiquitination-proteasomal degradation, and transcription activation. *Mol Pharmacol*, *76*(6), 1265-78.

[96] Giles, N. M., Watts, A. B., Giles, G. I., Fry, F. H., Littlechild, J. A., & Jacob, C. (2003). Metal and redox modulation of cysteine protein function. *Chem Biol*, *10*(8), 677-93.

[97] Lin, H., Su, X., & He, B. (2012). Protein lysine acylation and cysteine succination by intermediates of energy metabolism. *ACS Chem Biol*, *7*(6), 947-60.

[98] He, X., & Ma, Q. (2010). Critical Cysteine Residues of Kelch-Like ECH-Associated Protein 1 in Arsenic Sensing and Suppression of Nuclear Factor Erythroid 2-Related Factor 2. *J Pharmacol Exp Ther*, *332*(1), 66–75.

[99] Benhar, M., Forrester, M. T., & Stamler, J. S. (2009). Protein denitrosylation: enzymatic mechanisms and cellular functions. *Nat Rev Mol Cell Biol*, *10*(10), 721-32.

[100] Lipton, S. A., Singel, D. J., & Stamler, J. S. (1994). Nitric oxide in the central nervous system. *Prog Brain Res*, *103*, 359-64.

[101] Stamler, J. S., Toone, E. J., Lipton, S. A., & Sucher, N. J. (1997). (S)NO

Signals: translocation, regulation and a concensus motif. *Neuron*, *18*(5), 691-6.

[102] Dawson, V. L., & Sawson, T. M. (1998). Nitric oxide in neurodegeneration. *Prog Brain Res*, *118*, 215-229.

[103] Foster, M. W., Hess, D. T., & Stamler, J. S. (2009). Protein S-nitrosylation in health and disease: a current perspective. *Trends Mol Med*, *15*(9), 391-404.

[104] Nakamura, T., & Lipton, S. A. (2009). Cell death: protein misfolding and neurodegenerative diseases. *Apoptosis*, *14*(4), 455-68.

[103] Gu, Z., Nakamura, T., & Lipton, S. A. (2010). Redox reactions induced by nitrosative stress mediate protein misfolding and mitochondrial dysfunction in neurodegenerative diseases. *Mol Neurobiol*, *41*(2-3), 55-72.

[106] Bredt, D. S., Hwang, P. M., Glatt, C. E., Lowenstein, C., Reed, R. R., & Snyder, S. H. (1991). Cloned and expressed nitric oxide synthase structurally resembles cytochrome P-450 reductase. *Nature*, *351*(6329), 714–8.

[107] Garthwaite, J., Charles, S. L., & Chess, W. R. (1988). Endothelium-derived relaxing factor release on activation of NMDA receptors suggests role as intercellular messenger in the brain. *Nature*, *336*(6197), 385–8.

[108] Beal, M. F. (2001). Experimental models of Parkinson's disease. *Nat Rev Neurosci*, *2*(5), 325–34.

[109] Zhao, Q. F., Yu, J. T., & Tan, L. (2014). S-Nitrosylation in Alzheimer's disease. *Mol Neurobiol*, doi: 10.1007/s12035-014-8672-2.

[110] Cho, D. H., Nakamura, T., Fang, J., Cieplak, P., Godzik, A., Gu, Z., et al. (2009). S-Nitrosylation of Drp1 mediates beta-amyloid-related mitochondrial fission and neuronal injury. *Science*, *324*(5923), 102–5.

[111] Ho, G. P., Selvakumar, B., Mukai, J., Hester, L. D., Wang, Y., Gogos, J. A., & Snyder, S. H. (2011). S-Nitrosylation and S-palmitoylation reciprocally regulate synaptic targeting of PSD-95. *Neuron*, *71*(1), 131–41.

[112] Malito, E., Ralat, L. A., Manolopoulou, M., Tsay, J. L., Wadlington, N. L., & Tang, W. J. (2008). Molecular bases for the recognition of short peptide substrates and cysteine-directed modifications of human insulin-degrading enzyme. *Biochemistry*, *47*(48), 12822-34.

[113] Cordes, C. M., Bennett, R. G., Siford, G. L., & Hamel, F. G. (2009). Nitric oxide inhibits insulin-degrading enzyme activity and function through S-nitrosylation. *Biochem Pharmacol*, *77*(6), 1064-73.

[114] Kruszelnicka, O. (2014) Nitric oxide vs insulin secretion, action and clearance. *Diabetologia*, *57*(1), 257–8.

[115] Ghebranious, N., Ivacic, L., Mallum, J., & Dokken, C. (2005). Detection of

ApoE E2, E3 and E4 alleles using MALDI-TOF mass spectrometry and the homogeneous mass-extend technology. *Nucleic Acids Res, 33*(17), e149.

[116] Jiang, Q., Lee, C. Y., Mandrekar, S., Wilkinson, B., Cramer, P., Zelcer, N., et al. (2008). ApoE promotes the proteolytic degradation of Aβ. *Neuron, 58*(5), 681–93.

[117] Abrams, A. J., Farooq, A., & Wang, G. (2011). S-nitrosylation of ApoE in Alzheimer's disease. *Biochemistry, 50*(17), 3405-7.

[118] Westermann, B. (2002). Merging mitochondria matters: Cellular role and molecular machinery of mitochondrial fusion. *EMBO Rep, 3*(6), 527–31.

[119] Youle, R. J., & Karbowski, M. (2005). Mitochondrial fission in apoptosis. *Nat Rev Mol Cell Biol, 6*(8), 657–63.

[120] Barsoum, M. J., Yuan, H., Gerencser, A. A., Liot, G., Kushnareva, Y., Graber, S., et al. (2006). Nitric oxide-induced mitochondrial fission is regulated by dynamin-related GTPases in neurons. *EMBO J, 25*(16), 3900-11.

[121] Wang, X., Su, B., Siedlak, S. L., Moreira, P. I., Fujioka, H., Wang, Y., et al. (2008). Amyloid-β overproduction causes abnormal mitochondrial dynamics via differential modulation of mitochondrial fission/fusion proteins. *Proc Natl Acad Sci USA, 105*(49), 19318–23.

[122] Nakamura, T., & Lipton, S. A. (2011). S-nitrosylation of critical protein thiols mediates protein misfolding and mitochondrial dysfunction in neurodegenerative diseases. *Antioxid Redox Signal, 14*(8), 1479-92.

[123] Cho, D. H., Nakamura, T., Fang, J., Cieplak, P., Godzik, A., Gu, Z., et al. (2009). S-Nitrosylation of Drp1 Mediates β-Amyloid–Related Mitochondrial Fission and Neuronal Injury. *Science, 324*(5923), 102-5.

[124] Lyles, M. M. & Gilbert, H. F. (1991). Catalysis of the oxidative folding of ribonuclease A by protein disulfide isomerase: pre-steady-state kinetics and the utilization of the oxidizing equivalents of the isomerase. *Biochemistry, 30*(3), 619–25.

[125] Akhtar, M. W., Sunico, C. R., Nakamura, T., & Lipton, S. A. (2012). Redox Regulation of Protein Function via Cysteine S-Nitrosylation and Its Relevance to Neurodegenerative Diseases. *Int J Cell Biol, 2012*, 463756.

[126] Uehara, T., Nakamura, T., Yao, D., Shi, Z. Q., Gu, Z., Ma, Y., et al. (2006). S-nitrosylated protein-disulphide isomerase links protein misfolding to neurodegeneration. *Nature, 441*(7092), 513-7.

[127] Ohshima, T., Ward, J. M., Huh, C. G., Longenecker, G., Veeranna, Pant, H. C., et al. (1996). Targeted disruption of the cyclin-dependent kinase 5 gene

results in abnormal corticogenesis, neuronal pathology and perinatal death. *Proc Natl Acad Sci USA*, *93*(20), 11173-8.

[128] Xie, Z., Sanada, K., Samuels, B. A., Shih, H., & Tsai, L. H. (2003). Serine 732 phosphorylation of FAK by Cdk5 is important for microtubule organization, nuclear movement, and neuronal migration. *Cell*, *114*(4), 469–82.

[129] Kim, Y., Sung, J. Y., Ceglia, I., Lee, K. W., Ahn, J. H., Halford, J. M., et al. (2006). Phosphorylation of WAVE1 regulates actin polymerization and dendritic spine morphology. *Nature*, *442*(7104), 814-7.

[130] Wang, J., Liu, S., Fu, Y., Wang, J. H., & Lu, Y. (2003). Cdk5 activation induces hippocampal CA1 cell death by directly phosphorylating NMDA receptors. *Nat Neurosci*, *6*(10), 1039-47.

[131] Zaręba, K. M., Szwajda, A., Dadlez, M., Wysłouch, C. A., & Lalowski, M. (2014). Global analysis of S-nitrosylation sites in the wild type (APP) transgenic mouse brain-clues for synaptic pathology. *Mol Cell Proteomics*, *13*(9), 2288-305.

[132] Schuldiner, S., Shirvan, A., & Linial, M. (1995). Vesicular neurotransmitter transporters: from bacteria to humans. *Physiol Rev*, *75*(2), 369–92.

[133] Moriyama, Y., & Yamamoto, A. (2004). Glutamatergic chemical transmission: look! Here there, and anywhere. *J Biochem*, *135*(2), 155-63.

[134] Blakely, R. D., & Edwards, R. H. (2012). Vesicular and plasma membrane transporters for neurotransmitters. *Cold Spring Harb Perspect Biol*, *4*(2), pii: a005595.

[135] Moechars, D., Weston, M. C., Leo, S., Callaerts, V. Z., Goris, I., Daneels, G., et al. (2006). Vesicular glutamate transporter VGLUT2 expression levels control quantal size and neuropathic pain. *J Neurosci*, *26*(46), 12055-66.

[136] Mitew, S., Kirkcaldie, M. T., Dickson, T. C., & Vickers, J. C. (2013). Altered synapses and gliotransmission in Alzheimer's disease and AD model mice. *Neurobiol Aging*, *34*(10), 2341-51.

[137] Cassano, T., Serviddio, G., Gaetani, S., Romano, A., Dipasquale, P., Cianci S., et al. (2012). Glutamatergic alterations and mitochondrial impairment in a murine model of Alzheimer disease. *Neurobiol Aging*, *33*(6), 1121.e1-12.

[138] Kirvell, S. L., Esiri, M., & Francis, P. T. (2006). Down-regulation of vesicular glutamate transporters precedes cell loss and pathology in Alzheimer's disease. *J Neurochem*, *98*(3), 939-50.

[139] Canas, P. M., Simões, A. P., Rodrigues, R. J., & Cunha, R. A. (2014). Predominant loss of glutamatergic terminal markers in a β-amyloid peptide

model of Alzheimer's disease. *Neuropharmacology*, *76*(Pt A), 51-6.

[140] Chen, K. H., Reese, E. A., Kim, H. W., Rapoport, S. I., & Rao, J. S. (2011). Disturbed neurotransmitter transporter expression in Alzheimer's disease brain. *J Alzheimers Dis*, *26*(4), 755-66.

[141] Zhang, H., Zhang, Y., Xu, H., Wang, L., Zhao, J., Wang, J., et al. (2013). Locomotor activity and anxiety status, but not spatial working memory, are affected in mice after brief exposure to cuprizone. *Neurosci Bull*, *29*(5), 633-41.

[142] Che, Y., Cui, Y. H., Tan, H., Andreazza, A. C., Young, L. T., & Wang, J. F. (2013). Abstinence from repeated amphetamine treatment induces depressive like behaviors and oxidative damage in rat brain. *Psychopharmacology*, *227*(4), 605-14.

[143] Zhu, S., Wang, H., Shi, R., Zhang, R., Wang, J., Kong, L., et al. (2014). Chronic Phencyclidine Induces Inflammatory Responses and Activates GSK3β in Mice. *Neurochem Res*, *39*(12), 2385-93.

[144] Zhu, S., He, J., Zhang, R., Kong, L., Tempier, A., Kong, J., et al. (2013). Therapeutic effects of quetiapine on memory deficit and brain betaamyloid plaque pathology in a transgenic mouse model of Alzheimer's disease. *Curr Alzheimer Res*, *10*(3), 270–8.

[145] Vorhees, C. V., & Williams, M. T. (2006). Morris water maze: procedures for assessing spatial and related forms of learning and memory. *Nat Protoc*, *1*(2), 848-58.

[146] Chu, P. W., Hadlock, G. C., Vieira, B. P., Stout, K., Hanson, G. R., & Fleckenstein, A. E. (2010) Methamphetamine alters vesicular monoamine transporter-2 function and potassium-stimulated dopamine release. *J Neurochem*, *115*(2), 325-32.

[147] Morland, C., Nordengen, K., Larsson, M., Prolo, L. M., Farzampour, Z., Reimer R. J, et al. (2013) Vesicular uptake and exocytosis of L-aspartate is independent of sialin. *FASEB J*, *27*(3), 1264-74.

[148] Varoqui, H., & Erickson, J. D. (1996) Active transport of acetylcholine by the human vesicular acetylcholine transporter. *J Biol Chem*, *271*(44), 27229-32.

[149] Jaffrey, S. R., & Snyder, S. H. (2001). The Biotin Switch Method for the Detection of S-Nitrosylated Proteins. *Sci STKE*, 2001(86), pl1.

[150] Murray, C. I., Kane, L. A., Uhrigshardt, H., Wang, S. B., & Van, E. J. E. (2011). Site-mapping of in vitro S-nitrosation in cardiac mitochondria: implications for cardioprotection. *Mol Cell Proteomics*, *10*(3), M110.004721.

[151] Dinnendahl, V., & Stock, K. (1975). Effects of arecoline and cholinesterase

inhibitors on cyclic guanosine 3',5'-monophosphate and adenosine 3'.5'-monophosphate in mouse brain. *Naunyn Schmiedebergs Arch Pharmacol*, *290*(2-3), 297-306.

[152] Masson, J., Sagné, C., Hamon, M., & El Mestikawy, S. (1999). Neurotransmitter transporters in the central nervous system. *Pharmacol Rev*, *51*(3), 439-64.

[153] Sheng, M., Sabatini, B. L., & Südhof, T. C. (2012). Synapses and Alzheimer's disease. *Cold Spring Harb Perspect Biol*, *4*(5), pii: a005777.

[154] Chaudhry, F. A., Reimer, R. J., Krizaj, D., Barber, D., Storm, M. J., Copenhagen, D. R., et al. (1999). Molecular analysis of system N suggests novel physiological roles in nitrogen metabolism and synaptic transmission. *Cell*, *99*(7), 769-80.

[155] Krantz, D. E., Waites, C., Oorschot, V., Liu, Y., Wilson, R. I., Tan, P. K., et al. (2000). A phosphorylation site regulates sorting of the vesicular acetylcholine transporter to dense core vesicles. *J Cell Biol*, *149*(2), 379-96.

[156] Uniprot Org

[157] Thiriot, D. S., & Ruoho, A. E. (2001). Mutagenesis and derivatization of human vesicle monoamine transporter 2 (VMAT2) cysteines identifies transporter domains involved in tetrabenazine binding and substrate transport. *J Biol Chem*, *276*(29), 27304-15.

[158] Fei H., Karnezis, T., Reimer, R. J., & Krantz, D. E. (2007). Membrane topology of the Drosophila vesicular glutamate transporter. *J Neurochem*, *101*(6), 1662-71.

[159] Thiriot, D. S., Sievert, M. K., & Ruoho, A. E. (2002). Identification of human vesicle monoamine transporter (VMAT2) lumenal cysteines that form an intramoleculardisulfide bond. *Biochemistry*, *41*(20), 6346-53.

[160] Kaye, D. M., Gruskin, S., Smith, A. I., & Elser, M. D. (2000). Nitric oxide mediated modulation of norepinephrine transport: identification of a potential target for S-nitrosylation. *Br J Pharmacol*, *130*(5), 1060-4.

[161] Keil, U., Bonert, A., Marques, C. A., Scherping, I., Weyermann, J., Strosznajder, J. B., et al. (2004). Amyloid beta-induced changes in nitric oxide production and mitochondrial activity lead to apoptosis. *J Biol Chem*, *279*(48), 50310-20.

[162] Cetin, F., Yazihan, N., Dincer, S., & Akbulut, G. (2013). The effect of intracerebroventricular injection of beta amyloid peptide (1-42) on caspase-3 activity, lipid peroxidation, nitric oxide and NOS expression in young adult and aged rat brain. *Turk Neurosurg*, *23*(2), 144-50.

[163] Diaz, A., Limon, D., Chávez, R., Zenteno, E., & Guevara, J. (2012). Aβ25-35

injection into the temporal cortex induces chronic inflammation that contributes to neurodegeneration and spatial memory impairment in rats. *J Alzheimers Dis*, *30*(3), 505-22.

[164] Molokanova, E., Akhtar, M. W., Sanz-Blasco, S., Tu, S., Piña-Crespo, J. C., McKercher, S. R., et al. (2014). Differential effects of synaptic and extrasynaptic NMDA receptors on Aβ-induced nitric oxide production in cerebrocortical neurons. *J Neurosci*, *34*(14), 5023-8.

[165] Eyerman, D. J., & Yamamoto, B. K. (2007)。 A rapid oxidation and persistent decrease in the vesicular monoamine transporter 2 after methamphetamine. *J Neurochem*, *103*(3), 1219-27.

[171] Tucci, P., Mhillaj, E., Morgese, M. G., Colaianna, M., Zotti. M., Schiavone. S., et al. (2014). Memantine prevents memory consolidation failure induced by soluble beta amyloid in rats. *Front Behav Neurosci*, *8*, 332.

[172] Varga, E., Juhász, G., Bozsó, Z., Penke, B., Fülöp, L., & Szegedi, V. (2014). Amyloid-β1-42 Disrupts Synaptic Plasticity by Altering Glutamate Recycling at the Synapse. *J Alzheimers Dis*. [Epub ahead of print]

[173] Pereira, A. C., Lambert, H. K., Grossman, Y. S., Dumitriu, D., Waldman, R., Jannetty, S. K., et al. (2014) Glutamatergic regulation prevents hippocampal dependent age-related cognitive decline through dendritic spine clustering. *Proc Natl Acad Sci USA*, *111*(52), 18733-8.

[174] Hascup, K. N., & Hascup, E. R. (2014). Altered Neurotransmission Prior to Cognitive Decline in AβPP/PS1 Mice, a Model of Alzheimer's Disease. *J Alzheimers Dis*. [Epub ahead of print]

[175] Tucci, P., Mhillaj, E., Morgese, M. G., Colaianna, M., Zotti, M., Schiavone, S., et al. (2014). Memantine prevents memory consolidation failure induced by soluble beta amyloid in rats. *Front Behav Neurosci*, *8*, 332.

[176] Gebhardt, C., Körner, R., & Heinemann, U. (2002). Delayed anoxic depolarizations in hippocampal neurons of mice lacking the excitatory amino acid carrier 1. *Cereb Blood Flow Metab*, *22*(5), 569-75.

[177] Vandenberg R. J., & Ryan R. M. (2013). Mechanisms of Glutamate Transport. *Physiological Reviews*, *93*(4), 1621-57.

[178] Choi, D. Y., Lee, Y. J., Hong, J. T., & Lee, H. J. (2012). Antioxidant properties of natural polyphenols and their therapeutic potentials for Alzheimer's disease. *Brain Res Bull*, *87*(2-3), 144-53.

[179] Fu, X., Zhang, J., Guo, L., Xu, Y., Sun, L., Wang, S., et al. (2014). Protective role of luteolin against cognitive dysfunction induced by chronic cerebral

hypoperfusion in rats. *Pharmacol Biochem Behav, 126*: 122-30.

[180] Brondino, N., Re, S., Boldrini, A., Cuccomarino, A., Lanati, N., Barale, F., et al. (2014). Curcumin as a therapeutic agent in dementia: a mini systematic review of human studies. *Scientific World Journal*, *2014*, 174282.

[181] Zhang, S. Q., Sawmiller, D., Li, S., Rezai, Z. K., Hou, H., Zhou, S., et al. (2013). Octyl gallate markedly promotes anti-amyloidogenic processing of APP through estrogen receptor-mediated ADAM10 activation. *PLoS One*, *8*(8), e71913.

[182] Lee, Y. W., Kim, D. H., Jeon, S. J., Park, S. J., Kim, J. M., Jung, J. M., et al. (2013). Neuroprotective effects of salvianolic acid B on an Aβ25-35 peptide-induced mouse model of Alzheimer's disease. *Eur J Pharmacol, 704*(1-3), 70-7.

[183] Perrella, J., & Bhavnani, B. R. (2005). Protection of cortical cells by equine estrogens against glutamate-induced excitotoxicity is mediated through a calcium independent mechanism. *BMC Neurosci*, *6*, 34.

[184] Greco, R., Amantea, D., Blandini, F., Nappi, G., Bagetta, G., Corasaniti, M. T., et al. (2007). Neuroprotective effect of nitroglycerin in a rodent model of ischemic stroke: evaluation of Bcl-2 expression. *Int Rev Neurobiol*, *82*, 423-35.

[185] Javed, H., Khan, M. M., Ahmad, A., Vaibhav, K., Ahmad, M. E., Khan, A., et al. (2012). Rutin prevents cognitive impairments by ameliorating oxidative stress and neuroinflammation in rat model of sporadic dementia of Alzheimer type. *Neuroscience, 210*, 340-52.

[186] Perluigi, M., Joshi, G., Sultana, R., Calabrese, V., De, M. C., Coccia, R., et al. (2006). In vivo protective effects of ferulic acid ethyl ester against amyloid-beta peptide 1-42-induced oxidative stress. *J Neurosci Res*, *84*(2), 418-26.

[187] Vámos, E., Párdutz, A., Varga, H., Bohár, Z., Tajti, J., Fülöp, F., et al. (2009). l-kynurenine combined with probenecid and the novel synthetic kynurenic acid derivative attenuate nitroglycerin-induced nNOS in the rat caudal trigeminal nucleus. *Neuropharmacology*, *57*(4), 425-429.

[188] Talantova, M., Sanz, B. S., Zhang, X., Xia, P., Akhtar, M. W., Okamoto, S., et al. (2013). Aβ induces astrocytic glutamate release, extrasynaptic NMDA receptor activation, and synaptic loss. *Proc Natl Acad Sci USA*, *110*(27), E2518-2527.